SUPPLEMENT TO "INEQUALITY, BUSINESS CYCLES, AND MONETARY-FISCAL POLICY"

(*Econometrica*, Vol. 89, No. 6, November 2021, 2559–2599)

ANMOL BHANDARI
Economics Department, University of Minnesota

DAVID EVANS
Economics Department, University of Oregon

MIKHAIL GOLOSOV
Economics Department, University of Chicago

THOMAS J. SARGENT
Economics Department, New York University

APPENDIX A: ADDITIONAL DETAILS FOR SECTION 3

WE FILL IN THE MISSING STEPS for Section 3. First, in Section A.1, we show how to formulate the Ramsey problem recursively, then in the context of the Section 3.1 economy, how our method extends to higher-order approximations. Second, we show how to generalize the expansions so that we can deal with persistent aggregate and idiosyncratic shocks as well as additional state variables, as discussed in Section 3.2.

A.1. *Recursive Formulation of the Ramsey Problem*

Here, we show that the Lagrangian in equation (21) in Section 3 of the main text admits a recursive solution from $t \geq 1$. We will also describe the F and R mappings that appear in equations (22) and (23) in this case. For completeness, we repeat the maximization problem here and list all implementability constraints. Given $\{b_{i,-1}\}_i$ and $\mu_{i,-1} = 0$, the planning problem is

$$\inf \sup \mathbb{E}_0 \sum_{t=0}^{\infty} \beta^t \int \Big[u(c_{i,t}, n_{i,t}) + \big(u_{c,i,t} c_{i,t} + u_{n,i,t} n_{i,t} - u_{c,i,t}\big\{T_t + \big(1 - \Upsilon_t^d\big) D_t\big\}\big)\mu_{i,t} + \left(\frac{1 - \Upsilon_t^b}{1 + \Pi_t}\right) b_{i,t-1} u_{c,i,t} (\mu_{i,t-1} - \mu_{i,t}) \Big] di$$

subject to

$$Q_{t-1} M_{t-1} = \beta m_{i,t-1}^{-1} \mathbb{E}_{t-1} \big[u_{c,i,t} \big(1 - \Upsilon_t^b\big) (1 + \Pi_t)^{-1} \big], \tag{41a}$$

$$u_{c,i,t} W_t \big(1 - \Upsilon_t^n\big) \mathcal{E}_t \varepsilon_{,i,t} = -u_{n,i,t}, \tag{41b}$$

$$M_t = m_{i,t}^{-1} u_{c,i,t}, \tag{41c}$$

Anmol Bhandari: bhandari@umn.edu
David Evans: devans@uoregon.edu
Mikhail Golosov: golosov@uchicago.edu
Thomas J. Sargent: ts43@nyu.edu

 https://doi.org/10.3982/ECTA16414

$$\int u_{c,i,t}\,di = M_t, \tag{41d}$$

$$\int c_{i,t}\,di = C_t, \tag{41e}$$

$$C_t + \bar{G} = \int \mathcal{E}_t \varepsilon_{,i,t} n_{i,t}\,di - \frac{\psi}{2}\Pi_t^2, \tag{41f}$$

$$D_t = (1 - W_t)\int \mathcal{E}_t \varepsilon_{,i,t} n_{i,t}\,di - \frac{\psi}{2}\Pi_t^2. \tag{41g}$$

First-Order Conditions. Let $\beta^{t-1}\rho_{i,t-1}$, $\beta^t\phi_{i,t}$, $\beta^t\varphi_{i,t}$ be Lagrange multipliers on household-level constraints (41a)–(41c); let $\beta^t\lambda_t$, $\beta^t\chi_t$, $\beta^t\Xi_t$, $\beta^t\zeta_t$ be Lagrange multipliers on aggregate constraints (41d)–(41g). First-order conditions with respect to household-level variables: $b_{i,t-1}$, $c_{i,t}$, $n_{i,t}$, $m_{i,t}^{-1}$, $\mu_{i,t}$ are

$$0 = \mathbb{E}_{t-1}\left(\frac{1-\Upsilon_t^b}{1+\Pi_t}\right)u_{c,i,t}(\mu_{i,t-1} - \mu_{i,t}), \tag{42a}$$

$$\begin{aligned} 0 = {} & \mu_{i,t}(u_{cc,i,t}\big[c_{i,t} - \big(T_t + \big(1-\Upsilon_t^d\big)D_t\big] + u_{c,i,t}) + \left(\frac{1-\Upsilon_t^b}{1+\Pi_t}\right)b_{i,t-1}u_{cc,i,t}(\mu_{i,t-1} - \mu_{i,t}) \\ & - \phi_{i,t}W_t\big(1-\Upsilon_t^n\big)\epsilon_{i,t}u_{cc,i,t} + \rho_{i,t-1}m_{i,t-1}^{-1}\big(1-\Upsilon_t^b\big)(1+\Pi_t)^{-1}u_{cc,i,t} \\ & + \varphi_{i,t}u_{cc,it}m_{i,t}^{-1} - \chi_t - \lambda_t + u_{c,i,t}, \end{aligned} \tag{42b}$$

$$0 = u_{n,i,t} + \mu_{i,t}(u_{nn,i,t}n_{i,t} + u_{n,i,t}) - \phi_{i,t}u_{nn,i,t} + \big[\Xi_t + \zeta_t(1-W_t)\big]\mathcal{E}_t\varepsilon_{,i,t}, \tag{42c}$$

$$0 = \beta\mathbb{E}_t\big[\rho_{i,t}u_{c,i,t+1}\big(1-\Upsilon_{t+1}^b\big)(1+\Pi_{t+1})^{-1}\big] + \varphi_{i,t}u_{c,it}, \tag{42d}$$

$$\begin{aligned} 0 = {} & \big(u_{c,i,t}c_{i,t} + u_{n,i,t}n_{i,t} - u_{c,i,t}\big\{T_t + \big(1-\Upsilon_t^d\big)D_t\big\}\big) \\ & - \left(\frac{1-\Upsilon_t^b}{1+\Pi_t}\right)b_{i,t-1}u_{c,i,t} + \beta\mathbb{E}_t\left(\frac{1-\Upsilon_{t+1}^b}{1+\Pi_{t+1}}\right)b_{i,t}u_{c,i,t+1}. \end{aligned} \tag{42e}$$

First-order conditions with respect to aggregate variables C_t, D_t, M_t, Q_t, W_t, $(1+\Pi_t)^{-1}$, and T_t, Υ_t^d, Υ_t^b, Υ_t^n are

$$0 = \chi_t - \Xi_t, \tag{43a}$$

$$0 = -\big(1-\Upsilon_t^d\big)\int u_{c,i,t}\mu_{i,t}\,di - \zeta_t, \tag{43b}$$

$$0 = -\int \rho_{i,t}Q_t - \int \varphi_{i,t}\,di + \lambda_t, \tag{43c}$$

$$0 = -\int \rho_{i,t-1}\,di, \tag{43d}$$

$$0 = -\int \phi_{i,t}u_{c,i,t}\big(1-\Upsilon_t^n\big)\mathcal{E}_t\varepsilon_{,i,t}\,di - \zeta_t\int \mathcal{E}_t\varepsilon_{,i,t}n_{i,t}\,di, \tag{43e}$$

$$0 = \big(1-\Upsilon_t^b\big)\int b_{i,t-1}u_{c,i,t}(\mu_{i,t-1} - \mu_{i,t})\,di + \psi\Pi_t(1+\Pi_t)^2(\Xi_t + \zeta_t)$$

$$+\beta\left(1-\Upsilon_t^b\right)\int \rho_{i,t-1}m_{i,t-1}^{-1}u_{c,i,t}\,di, \tag{43f}$$

$$0=\int u_{c,i,t}\mu_{i,t}\,di, \tag{43g}$$

$$0=\int u_{c,i,t}\mu_{i,t}\,di, \tag{43h}$$

$$0=-\int b_{i,t-1}u_{c,i,t}(\mu_{i,t-1}-\mu_{i,t})\,di-\beta\int \rho_{i,t-1}m_{i,t-1}^{-1}u_{c,i,t}\,di, \tag{43i}$$

$$0=W_t\int \phi_{i,t}u_{c,i,t}\mathcal{E}_t\varepsilon_{,i,t}. \tag{43j}$$

We can simplify some equations. We can set $\Pi_t=\zeta_t=0$ and define $\hat{T}_t\equiv T_t+(1-\Upsilon_t^d)D_t$ and ignore (43f). Solving equations (42a)–(43j) is then the same as solving the following equations:

$$0=\mathbb{E}_{t-1}\left(1-\Upsilon_t^b\right)u_{c,i,t}(\mu_{i,t-1}-\mu_{i,t}), \tag{44a}$$

$$\begin{aligned}0=&\mu_{i,t}\left(u_{cc,i,t}[c_{i,t}-\hat{T}_t]+u_{c,i,t}\right)+\left(1-\Upsilon_t^b\right)b_{i,t-1}u_{cc,i,t}(\mu_{i,t-1}-\mu_{i,t})\\&-\phi_{i,t}W_t\left(1-\Upsilon_t^n\right)\epsilon_{i,t}u_{cc,i,t}+\rho_{i,t-1}m_{i,t-1}^{-1}\left(1-\Upsilon_t^b\right)u_{cc,i,t}\\&+\varphi_{i,t}u_{cc,it}m_{i,t}^{-1}-\Xi_t-\lambda_t+u_{c,i,t},\end{aligned} \tag{44b}$$

$$0=u_{n,i,t}+\mu_{i,t}(u_{nn,i,t}n_{i,t}+u_{n,i,t})-\phi_{i,t}u_{nn,i,t}+\Xi_t\epsilon_{i,t}, \tag{44c}$$

$$0=\beta\mathbb{E}_t\left[\rho_{i,t}u_{c,i,t+1}\left(1-\Upsilon_{t+1}^b\right)\right]+\varphi_{i,t}u_{c,it}, \tag{44d}$$

$$\begin{aligned}0=&u_{c,i,t}c_{i,t}+u_{n,i,t}n_{i,t}-u_{c,i,t}\hat{T}_t,\\&-\left(1-\Upsilon_t^b\right)b_{i,t-1}u_{c,i,t}+\beta\mathbb{E}_t\left(1-\Upsilon_t^b\right)b_{i,t}u_{c,i,t+1},\end{aligned} \tag{44e}$$

$$0=-\int \varphi_{i,t}\,di+\lambda_t, \tag{44f}$$

$$0=\int \rho_{i,t-1}\,di, \tag{44g}$$

$$0=\int \phi_{i,t}u_{c,i,t}\epsilon_{i,t}\,di, \tag{44h}$$

$$0=\int b_{i,t-1}u_{c,i,t}(\mu_{i,t-1}-\mu_{i,t})\,di, \tag{44i}$$

$$0=\int u_{c,i,t}\mu_{i,t}\,di. \tag{44j}$$

Recursive Ramsey Problems. For $t\geq 1$, define individual-level states

$$z_{i,t-1}\equiv(m_{i,t-1},\mu_{i,t-1}),$$

and the aggregate state as a joint distribution over $z_{i,t-1}$ to be denoted Ω_{t-1}; the individual-level choice variables as

$$\tilde{\boldsymbol{x}}_{i,t} \equiv (c_{i,t}, n_{i,t}, b_{i,t-1}, \rho_{i,t-1}, \phi_{i,t}, \varphi_{i,t}, \mu_{i,t}, m_{i,t}),$$

and the aggregate-level choice variables as

$$\tilde{\boldsymbol{X}}_t \equiv \big(C_t, D_t, Q_t, W_t, M_t, \hat{T}_t, \Upsilon_t^b, \Upsilon_t^n, \lambda_t, \Xi_t\big).$$

For $t \geq 1$, given Ω_{t-1} and shocks $(\mathcal{E}_t, \{\varepsilon_{,i,t}\}_i)$, functions $\tilde{\boldsymbol{X}}(\Omega, \boldsymbol{\mathcal{E}})$, $\tilde{\boldsymbol{x}}(z, \Omega, \boldsymbol{\varepsilon}, \boldsymbol{\mathcal{E}})$, in the main text are defined as solutions to 17 equations (41a)–(41g) and (44a)–(44j) to be solved for 17 unknowns $\tilde{\boldsymbol{x}}_{i,t}$ and $\boldsymbol{X}_t$. The collection of equations (41a)–(41g) constitutes the F mapping in the text, and the collection of equations (44a)–(44j) constitutes the R mapping in the text.

For $t = 0$, define vectors $\tilde{\boldsymbol{x}}_{i,0}$ and $\tilde{\boldsymbol{X}}_0$ as

$$\tilde{\boldsymbol{x}}_{i,0} \equiv (c_{i,0}, n_{i,0}, \phi_{i,0}, \varphi_{i,0}, \mu_{i,0}, m_{i,0}),$$
$$\tilde{\boldsymbol{X}}_0 \equiv \big(C_0, D_0, Q_0, W_0, M_0, \hat{T}_0, \Upsilon_0^b, \Upsilon_0^n, \lambda_0, \Xi_0\big).$$

Given an initial condition $\Omega_{-1}^b \equiv \{b_{i,-1}\}_i$ and shocks $(\mathcal{E}_0, \{\varepsilon_{,i,0}\}_i)$ the time-0 policy functions $\tilde{\boldsymbol{X}}_0(\Omega_{-1}^b, \boldsymbol{\mathcal{E}})$, $\tilde{\boldsymbol{x}}_0(b, \Omega_{-1}^b, \boldsymbol{\varepsilon}, \mathcal{E})$ solve 15 equations (41b)–(41g), and (44b)–(44j) for 15 unknowns $\tilde{\boldsymbol{x}}_{i,0}$ and $\tilde{\boldsymbol{X}}_0$ given $\tilde{\boldsymbol{x}}_{i,1}$ and $\tilde{\boldsymbol{X}}_1$.

A.2. *Higher-Order Approximations for Section 3.1*

We start with a second-order approximation to the model presented in Section 3.1. These are given by

$$\begin{aligned}\tilde{\boldsymbol{X}}(\Omega, \sigma\boldsymbol{\mathcal{E}}; \sigma) = \bar{\boldsymbol{X}} &+ \sigma(\bar{\boldsymbol{X}}_{\boldsymbol{\mathcal{E}}}\boldsymbol{\mathcal{E}} + \bar{\boldsymbol{X}}_{\sigma}) \\ &+ \frac{1}{2}\sigma^2\big(\bar{\boldsymbol{X}}_{\boldsymbol{\mathcal{E}}\boldsymbol{\mathcal{E}}}.(\boldsymbol{\mathcal{E}}, \boldsymbol{\mathcal{E}}) + 2\bar{\boldsymbol{X}}_{\boldsymbol{\mathcal{E}}\sigma}\boldsymbol{\mathcal{E}} + \bar{\boldsymbol{X}}_{\sigma\sigma}\big) \\ &+ \mathcal{O}\big(\sigma^3\big),\end{aligned}$$

where the symbol $\mathsf{a} \cdot (\mathsf{b}, \mathsf{c})$ denotes a bilinear map.[32] A similar expansion can be written for $\tilde{\boldsymbol{x}}(z, \Omega, \sigma\boldsymbol{\varepsilon}, \sigma\boldsymbol{\mathcal{E}}; \sigma)$.

To obtain the necessary terms, we proceed in two steps: Section A.2.1 computes intermediate terms including higher-order Fréchet derivatives for individual and aggregate policy functions, and Section A.2.2 uses these terms to compute the second-order expansion. Although the second-order expansion requires additional notation, the steps below highlight how the the same fundamental insights presented in Section 3 maintain the tractability of the problem.

[32] Specifically, if a is a $n_1 \times n_2 \times n_3$ tensor, b is a $n_2 \times n_4$ matrix and c is a $n_3 \times n_5$ matrix then $\mathsf{d} = \mathsf{a} \cdot (\mathsf{b}, \mathsf{c})$ is $n_1 \times n_4 \times n_5$ tensor defined by

$$\mathsf{d}_{ilm} = \sum_{j,k} \mathsf{a}_{ijk}\mathsf{b}_{jl}\mathsf{c}_{km}.$$

This definition generalizes to when a, b, or c is infinite dimensional, such as with $\partial\bar{\boldsymbol{x}}_{\mathsf{z}}$.

A.2.1. *Intermediate Terms for Second-Order Expansions*

Differentiating equation (22) twice with respect to z, we find

$$\begin{aligned}0 = {} & \bar{F}_{x^-}\bar{\boldsymbol{x}}_{zz} + \bar{F}_{x}\bar{\boldsymbol{x}}_{zz} + \bar{F}_{x^+}(\bar{\boldsymbol{x}}_{zz} + \bar{\boldsymbol{x}}_z \mathsf{p} \bar{\boldsymbol{x}}_{zz}) \\ & + \bar{F}_{zz} + \bar{F}_{zx^-}\cdot(I, \bar{\boldsymbol{x}}_z) + \bar{F}_{zx}\cdot(I, \bar{\boldsymbol{x}}_z) + \bar{F}_{zx^+}\cdot(I, \boldsymbol{x}_z) \\ & + \bar{F}_{x^-z}\cdot(\bar{\boldsymbol{x}}_z, I) + \bar{F}_{x^-x^-}\cdot(\bar{\boldsymbol{x}}_z, \bar{\boldsymbol{x}}_z) + \bar{F}_{x^-x}\cdot(\bar{\boldsymbol{x}}_z, \bar{\boldsymbol{x}}_z) + \bar{F}_{x^-x^+}\cdot(\bar{\boldsymbol{x}}_z, \boldsymbol{x}_z) \\ & + \bar{F}_{xz}\cdot(\bar{\boldsymbol{x}}_z, I) + \bar{F}_{xx^-}\cdot(\bar{\boldsymbol{x}}_z, \bar{\boldsymbol{x}}_z) + \bar{F}_{xx}\cdot(\bar{\boldsymbol{x}}_z, \bar{\boldsymbol{x}}_z) + \bar{F}_{xx^+}\cdot(\bar{\boldsymbol{x}}_z, \boldsymbol{x}_z) \\ & + \bar{F}_{x^+z}\cdot(\bar{\boldsymbol{x}}_z, I) + \bar{F}_{x^+x^-}\cdot(\bar{\boldsymbol{x}}_z, \bar{\boldsymbol{x}}_z) + \bar{F}_{x^+x}\cdot(\bar{\boldsymbol{x}}_z, \bar{\boldsymbol{x}}_z) + \bar{F}_{x^+x^+}\cdot(\bar{\boldsymbol{x}}_z, \boldsymbol{x}_z),\end{aligned}$$

where I represents the identity matrix and we use $\mathsf{a}\cdot(\mathsf{b},\mathsf{c})$ to denote a bilinear map. Lines 2–5 appear complicated but are actually simply combining all of the already known derivatives of $\boldsymbol{x}$ with cross derivatives of F. It will prove convenient to combine all of these terms into a single term: $\sum_{\boldsymbol{\alpha},\boldsymbol{\beta}\in\{z,x^-,x,x^+\}}\bar{F}_{\boldsymbol{\alpha}\boldsymbol{\beta}}\cdot(\bar{\boldsymbol{\alpha}}_z, \bar{\boldsymbol{\beta}}_z)$ with the knowledge that $\bar{z}_z \equiv I$, $\bar{\boldsymbol{x}}_z^- \equiv \bar{\boldsymbol{x}}_z$, and $\bar{\boldsymbol{x}}_z^+ \equiv \bar{\boldsymbol{x}}_z$. In doing this, $\bar{\boldsymbol{x}}_{zz}$ can be represented by a simple linear equation

$$\bar{\boldsymbol{x}}_{zz} = -\big[\bar{F}_{x^-} + \bar{F}_x + \bar{F}_{x^+}(I + \bar{\boldsymbol{x}}_z \mathsf{p})\big]^{-1}\Bigg(\sum_{\boldsymbol{\alpha},\boldsymbol{\beta}\in\{z,x^-,x,x^+\}}\bar{F}_{\boldsymbol{\alpha}\boldsymbol{\beta}}\cdot(\bar{\boldsymbol{\alpha}}_z, \bar{\boldsymbol{\beta}}_z)\Bigg).$$

In a similar manner, one can show that

$$\partial \boldsymbol{x}_z \cdot \Delta = -\big[\bar{F}_{x^-} + \bar{F}_x + \bar{F}_{x^+}(I + \bar{\boldsymbol{x}}_z \mathsf{p})\big]^{-1}\Bigg(\sum_{\substack{\boldsymbol{\alpha}\in\{z,x^-,x,x^+\}\\ \boldsymbol{\beta}\in\{x^-,x,x^+,X\}}}\bar{F}_{\boldsymbol{\alpha}\boldsymbol{\beta}}\cdot(\bar{\boldsymbol{\alpha}}_z, \partial\bar{\boldsymbol{\beta}}\cdot\Delta)\Bigg),$$

where we use $\partial\bar{\boldsymbol{x}}^-\cdot\Delta \equiv \partial\bar{\boldsymbol{x}}^+\cdot\Delta \equiv \partial\bar{\boldsymbol{x}}\cdot\Delta$.

The last of the derivatives with respect to the state variables that are required for the second-order expansion is $\partial^2\bar{\boldsymbol{x}}\cdot(\Delta_1,\Delta_2)$. We will use the precomputed expressions for $\partial\bar{\boldsymbol{x}}$ and $\partial\bar{\boldsymbol{X}}$ evaluating them in the directions Δ_1 and Δ_2. Differentiating (22), we find

$$\begin{aligned}0 = {} & \bar{F}_{x^-}\partial^2\bar{\boldsymbol{x}}\cdot(\Delta_1,\Delta_2) + \bar{F}_x\partial^2\bar{\boldsymbol{x}}\cdot(\Delta_1,\Delta_2) + \bar{F}_{x^+}\big(\partial^2\bar{\boldsymbol{x}}\cdot(\Delta_1,\Delta_2) + \bar{\boldsymbol{x}}_z \mathsf{p}\,\partial^2\bar{\boldsymbol{x}}\cdot(\Delta_1,\Delta_2)\big) \\ & + \bar{F}_X\partial^2\bar{\boldsymbol{X}}\cdot(\Delta_1,\Delta_2) \\ & + \sum_{\boldsymbol{\alpha},\boldsymbol{\beta}\in\{x^-,x,x^+,X\}}\bar{F}_{\boldsymbol{\alpha}\boldsymbol{\beta}}\cdot(\partial\bar{\boldsymbol{\alpha}}\cdot\Delta_1, \partial\bar{\boldsymbol{\beta}}\cdot\Delta_2).\end{aligned}$$

In solving this equation for $\partial^2\bar{\boldsymbol{x}}\cdot(\Delta_1,\Delta_2)$, we find

$$\partial^2\bar{\boldsymbol{x}}\cdot(\Delta_1,\Delta_2) = \mathsf{A}(z,\Delta_1,\Delta_2) + \mathsf{C}(z)\partial^2\bar{X}\cdot(\Delta_1,\Delta_2),$$

where $\mathsf{A}(z,\Delta_1,\Delta_2)$ equals

$$-\big[\bar{F}_{x^-} + \bar{F}_x + \bar{F}_{x^+}(I + \bar{\boldsymbol{x}}_z \mathsf{p})\big]^{-1}\Bigg(\sum_{\boldsymbol{\alpha},\boldsymbol{\beta}\in\{x^-,x,x^+,X\}}\bar{F}_{\boldsymbol{\alpha}\boldsymbol{\beta}}\cdot(\partial\bar{\boldsymbol{\alpha}}\cdot\Delta_1, \partial\bar{\boldsymbol{\beta}}\cdot\Delta_2)\Bigg)$$

from terms already known and $\mathsf{C}(z)$ is the same term computed in Section 3.1. To find $\partial^2 \bar{\boldsymbol{X}} \cdot (\Delta_1, \Delta_2)$, we differentiate (23) to find

$$\begin{aligned} 0 = \bar{R}_x \int \partial^2 \bar{\boldsymbol{x}}(y) \cdot (\Delta_1, \Delta_2)\, d\Omega(y) + \bar{R}_X \partial^2 \bar{X} \cdot (\Delta_1, \Delta_2) \\ + \int \sum_{\boldsymbol{\alpha}, \boldsymbol{\beta} \in \{\boldsymbol{x}(y), X\}} \bar{R}_{\boldsymbol{\alpha}\boldsymbol{\beta}} \cdot (\partial \boldsymbol{\alpha} \cdot \Delta_1, \partial \boldsymbol{\beta} \cdot \Delta_2)\, d\Omega(y) \\ + \bar{R}_x \int \partial \bar{\boldsymbol{x}}(y) \cdot \Delta_1\, d\Delta_2(y) + \bar{R}_x \int \partial \bar{\boldsymbol{x}}(y) \cdot \Delta_2\, d\Delta_1(y). \end{aligned}$$

Plugging in for $\partial^2 \bar{\boldsymbol{x}} \cdot (\Delta_1, \Delta_2)$ yields a linear equation which can be easily solved for $\partial^2 \bar{\boldsymbol{X}} \cdot (\Delta_1, \Delta_2)$.

A.2.2. *Second-Order Expansions*

We can use these derivatives to compute the second-order terms. To find $\bar{\boldsymbol{x}}_{\boldsymbol{\varepsilon}\boldsymbol{\varepsilon}}$, differentiate F twice with respect to $\boldsymbol{\varepsilon}$ to get the linear equation[33]

$$0 = \bar{F}_x \bar{\boldsymbol{x}}_{\boldsymbol{\varepsilon}\boldsymbol{\varepsilon}} + \bar{F}_{x^+} \bar{\boldsymbol{x}}_z \mathsf{p} \bar{\boldsymbol{x}}_{\boldsymbol{\varepsilon}\boldsymbol{\varepsilon}} + \sum_{\boldsymbol{\alpha}, \boldsymbol{\beta} \in \{\boldsymbol{x}, \boldsymbol{x}^+, \boldsymbol{\varepsilon}\}} \bar{F}_{\boldsymbol{\alpha}\boldsymbol{\beta}} \cdot (\bar{\boldsymbol{\alpha}}_{\boldsymbol{\varepsilon}}, \bar{\boldsymbol{\beta}}_{\boldsymbol{\varepsilon}}),$$

where $\bar{\boldsymbol{x}}^+_{\boldsymbol{\varepsilon}} \equiv \bar{\boldsymbol{x}}_z \mathsf{p} \bar{\boldsymbol{x}}_{\boldsymbol{\varepsilon}}$ and $\boldsymbol{\varepsilon}_{\boldsymbol{\varepsilon}} \equiv I$. Similarly, $\bar{\boldsymbol{x}}_{\boldsymbol{\varepsilon}\boldsymbol{\mathcal{E}}}$ solves the following linear equation:

$$0 = \bar{F}_x \bar{\boldsymbol{x}}_{\boldsymbol{\varepsilon}\boldsymbol{\mathcal{E}}} + \bar{F}_{x^+} \bar{\boldsymbol{x}}_z \mathsf{p} \bar{\boldsymbol{x}}_{\boldsymbol{\varepsilon}\boldsymbol{\mathcal{E}}} + \sum_{\substack{\boldsymbol{\alpha} \in \{\boldsymbol{x}, \boldsymbol{x}^+, \boldsymbol{\varepsilon}\} \\ \boldsymbol{\beta} \in \{\boldsymbol{x}, \boldsymbol{x}^+, X, \boldsymbol{\mathcal{E}}\}}} \bar{F}_{\boldsymbol{\alpha}\boldsymbol{\beta}} \cdot (\bar{\boldsymbol{\alpha}}_{\boldsymbol{\varepsilon}}, \bar{\boldsymbol{\beta}}_{\boldsymbol{\mathcal{E}}}),$$

with the understanding that $\bar{\boldsymbol{\mathcal{E}}}_{\boldsymbol{\mathcal{E}}} \equiv I$ and $\bar{\boldsymbol{x}}^+_{\boldsymbol{\mathcal{E}}} \equiv \bar{\boldsymbol{x}}_z \mathsf{p} \bar{\boldsymbol{x}}_{\boldsymbol{\mathcal{E}}} + \partial \bar{\boldsymbol{x}} \cdot \bar{\Omega}_{\boldsymbol{\mathcal{E}}}$.

Differentiating twice with respect to $\boldsymbol{\mathcal{E}}$ yields

$$\begin{aligned} 0 = \bar{F}_x \bar{\boldsymbol{x}}_{\boldsymbol{\mathcal{E}}\boldsymbol{\mathcal{E}}} + \bar{F}_{x^+} (\bar{\boldsymbol{x}}_z \mathsf{p} \bar{\boldsymbol{x}}_{\boldsymbol{\mathcal{E}}\boldsymbol{\mathcal{E}}} + \partial \bar{\boldsymbol{x}} \cdot \bar{\Omega}_{\boldsymbol{\mathcal{E}}\boldsymbol{\mathcal{E}}}) + \bar{F}_X \bar{\boldsymbol{X}}_{EE} \\ + \bar{F}_{x^+} \big(\bar{\boldsymbol{x}}_{zz} \cdot (\mathsf{p} \bar{\boldsymbol{x}}_{\boldsymbol{\mathcal{E}}}, \mathsf{p} \bar{\boldsymbol{x}}_{\boldsymbol{\mathcal{E}}}) + \partial \bar{\boldsymbol{x}}_z \cdot (\mathsf{p} \bar{\boldsymbol{x}}_{\boldsymbol{\mathcal{E}}}, \bar{\Omega}_{\boldsymbol{\mathcal{E}}}) + \partial \bar{\boldsymbol{x}}_z \cdot (\bar{\Omega}_{\boldsymbol{\mathcal{E}}}, \mathsf{p} \bar{\boldsymbol{x}}_{\boldsymbol{\mathcal{E}}}) + \partial^2 \bar{\boldsymbol{x}} \cdot (\bar{\Omega}_{\boldsymbol{\mathcal{E}}}, \bar{\Omega}_{\boldsymbol{\mathcal{E}}}) \big) \\ + \sum_{\boldsymbol{\alpha}, \boldsymbol{\beta} \in \{\boldsymbol{x}, \boldsymbol{x}^+, X, \boldsymbol{\mathcal{E}}\}} \bar{F}_{\boldsymbol{\alpha}\boldsymbol{\beta}} \cdot (\bar{\boldsymbol{\alpha}}_{\boldsymbol{\mathcal{E}}}, \bar{\boldsymbol{\beta}}_{\boldsymbol{\mathcal{E}}}) \end{aligned} \tag{45}$$

and

$$\int \bar{R}_x \bar{\boldsymbol{x}}_{\boldsymbol{\mathcal{E}}\boldsymbol{\mathcal{E}}}(y) + \bar{R}_X \bar{X}_{\boldsymbol{\mathcal{E}}\boldsymbol{\mathcal{E}}} + \sum_{\boldsymbol{\alpha}, \boldsymbol{\beta} \in \{\bar{\boldsymbol{x}}(y), \bar{X}\}} \bar{R}_{\boldsymbol{\alpha}\boldsymbol{\beta}} \cdot (\bar{\boldsymbol{\alpha}}_{\boldsymbol{\mathcal{E}}}, \bar{\boldsymbol{\beta}}_{\boldsymbol{\mathcal{E}}})\, d\Omega(y). \tag{46}$$

All the terms in the second line can be computed from our analysis of the previous section and all the terms in the third line are known. What remains is to find $\bar{\boldsymbol{x}}_{\boldsymbol{\mathcal{E}}\boldsymbol{\mathcal{E}}}$ and $\bar{\boldsymbol{X}}_{\boldsymbol{\mathcal{E}}\boldsymbol{\mathcal{E}}}$. This requires us extend the steps we used in the proof of Theorem 1.

[33] For parsimony, we have dropped the dependence on z when not necessary.

Differentiating (24) twice with respect to $\boldsymbol{\mathcal{E}}$, evaluated at $\sigma = 0$, yields

$$\begin{aligned}\bar{\Omega}_{\boldsymbol{\mathcal{E}}\boldsymbol{\mathcal{E}}}(y) = &-\int \sum_i \delta(z^i - y^i) \prod_{j\neq i} \iota(z^j - y^j) \bar{z}^i_{\boldsymbol{\mathcal{E}}\boldsymbol{\mathcal{E}}}(z)\, d\Omega(z) \\ &- \int \sum_i \delta'(z^i - y^i) \prod_{j\neq i} \iota(z^j - y^j) \left[\bar{z}^i_{\boldsymbol{\mathcal{E}}}(z)\right]^2 d\Omega(z) \\ &+ \int \sum_i \delta(z^i - y^i) \sum_{j\neq i} \delta(z^j - y^j) \prod_{k\neq i,j} \iota(z^k - y^k) \bar{z}^j_{\boldsymbol{\mathcal{E}}}(z) \bar{z}^i_{\boldsymbol{\mathcal{E}}}(z)\, d\Omega(z).\end{aligned}$$

The density is then

$$\begin{aligned}\bar{\omega}_{\boldsymbol{\mathcal{E}}\boldsymbol{\mathcal{E}}}(y) &= \frac{\partial^{n_z}}{\partial \boldsymbol{y}^1 \partial \boldsymbol{y}^2 \cdots \partial \boldsymbol{y}^{n_z}} \bar{\Omega}_{\boldsymbol{\mathcal{E}}\boldsymbol{\mathcal{E}}}(y) \\ &= -\sum_i \frac{\partial}{\partial \boldsymbol{y}^i} \left(\bar{z}^i_{\boldsymbol{\mathcal{E}}\boldsymbol{\mathcal{E}}}(y) \omega_{\mathcal{E}}(y)\right) + \sum_i \sum_j \frac{\partial^2}{\partial \boldsymbol{y}^i \partial \boldsymbol{y}^j} \left(\bar{z}^i_{\boldsymbol{\mathcal{E}}}(y) \bar{z}^j_{\boldsymbol{\mathcal{E}}}(y) \omega_{\mathcal{E}}(y)\right).\end{aligned}$$

The identical steps to (1) then show that

$$\begin{aligned}&\partial \bar{\boldsymbol{x}}(z) \cdot \bar{\Omega}_{\boldsymbol{\mathcal{E}}\boldsymbol{\mathcal{E}}} \\ &\quad = \mathsf{C}(z) \partial \bar{\boldsymbol{X}} \cdot \bar{\Omega}_{\boldsymbol{\mathcal{E}}\boldsymbol{\mathcal{E}}} \equiv \mathsf{C}(z) \bar{\boldsymbol{X}}'_{\boldsymbol{\mathcal{E}}\boldsymbol{\mathcal{E}}}\end{aligned}$$

with $\bar{\boldsymbol{X}}'_{\boldsymbol{\mathcal{E}}\boldsymbol{\mathcal{E}}}$ equals

$$-\left(\bar{R}_x \int \mathsf{C}(y)\, d\Omega(y) + \bar{R}_X\right)^{-1} \bar{R}_x \left(\int \bar{\boldsymbol{x}}_z(y) \mathsf{p}\bar{\boldsymbol{x}}_{\boldsymbol{\mathcal{E}}\boldsymbol{\mathcal{E}}}(y) + \bar{\boldsymbol{x}}_{zz}(y) \cdot (\mathsf{p}\bar{\boldsymbol{x}}_{\mathcal{E}}, \mathsf{p}\bar{\boldsymbol{x}}_{\mathcal{E}})\, d\Omega(y)\right). \quad (47)$$

As with $\bar{\boldsymbol{X}}_{\boldsymbol{\mathcal{E}}}$, rather than solving for $\bar{\boldsymbol{x}}_{\boldsymbol{\mathcal{E}}\boldsymbol{\mathcal{E}}}(z)$ and $\bar{\boldsymbol{X}}_{\boldsymbol{\mathcal{E}}\boldsymbol{\mathcal{E}}}$ jointly, we substitute for $\partial \bar{\boldsymbol{x}}(z) \cdot \bar{\Omega}_{\boldsymbol{\mathcal{E}}\boldsymbol{\mathcal{E}}}$ in (45) and solve for $\bar{\boldsymbol{x}}_{\boldsymbol{\mathcal{E}}\boldsymbol{\mathcal{E}}}(z)$ yielding the linear relationship

$$\bar{\boldsymbol{x}}_{\boldsymbol{\mathcal{E}}\boldsymbol{\mathcal{E}}}(z) = \mathsf{D}_1(z) \cdot \begin{bmatrix} \bar{\boldsymbol{X}}_{\boldsymbol{\mathcal{E}}\boldsymbol{\mathcal{E}}} & \bar{\boldsymbol{X}}'_{\boldsymbol{\mathcal{E}}\boldsymbol{\mathcal{E}}} \end{bmatrix}^{\mathsf{T}} + \mathsf{D}_2(z),$$

where $\mathsf{D}_1(z)$ is identical to the D_1 in Section 3.1. We then use this relationship to substitute into equations (46) and (47) to find $\bar{\boldsymbol{X}}_{\boldsymbol{\mathcal{E}}\boldsymbol{\mathcal{E}}}$ and $\bar{\boldsymbol{X}}'_{\boldsymbol{\mathcal{E}}\boldsymbol{\mathcal{E}}}$.

A key part of the second-order approximations is capturing the effect of risk via the terms $\bar{\boldsymbol{x}}_{\sigma\sigma}(z)$ and $\bar{\boldsymbol{X}}_{\sigma\sigma}(z)$.[34] Let $\mathbb{C}_{\boldsymbol{\varepsilon}} \equiv \mathbb{E}\boldsymbol{\varepsilon}^{\intercal}\boldsymbol{\varepsilon}$ and $\mathbb{C}_{\mathcal{E}} \equiv \mathbb{E}\boldsymbol{\mathcal{E}}^{\intercal}\boldsymbol{\mathcal{E}}$ be the variance-covariance matrix of the idiosyncratic and aggregate shocks, respectively. Differentiating (22) and (23) yields[35]

$$\begin{aligned}0 = &\bar{F}_{x^-} (\bar{\boldsymbol{x}}_{\boldsymbol{\varepsilon}\boldsymbol{\varepsilon}} \cdot \mathbb{C}_{\boldsymbol{\varepsilon}} + \bar{\boldsymbol{x}}_{\boldsymbol{\mathcal{E}}\boldsymbol{\mathcal{E}}} \cdot \mathbb{C}_{\mathcal{E}}) + \bar{F}_x \bar{\boldsymbol{x}}_{\sigma\sigma} \\ &+ \bar{F}_X \bar{\boldsymbol{X}}_{\sigma\sigma} + \mathsf{F}_{x+} (\bar{\boldsymbol{x}}_{\boldsymbol{\varepsilon}\boldsymbol{\varepsilon}} \cdot \mathbb{C}_{\boldsymbol{\varepsilon}} + \bar{\boldsymbol{x}}_{\boldsymbol{\mathcal{E}}\boldsymbol{\mathcal{E}}} \cdot \mathbb{C}_{\mathcal{E}} + \bar{\boldsymbol{x}}_z \mathsf{p}\bar{\boldsymbol{x}}_{\sigma\sigma} + \partial \bar{\boldsymbol{x}} \cdot \bar{\Omega}_{\sigma\sigma}) \quad (48)\end{aligned}$$

[34] It is easy to verify that the cross derivatives with shocks and σ are zero.

[35] If a is a $n_1 \times n_2 \times n_2$ tensor and $\mathbb{C}$ is a $n_2 \times n_2$ matrix, then $\mathsf{d} = \mathsf{a} \cdot \mathbb{C}$ is length n_1 vector defined by

$$\mathsf{d}_i = \sum_{j,k} \mathsf{a}_{ijk} \mathbb{C}_{jk}.$$

and

$$0 = \bar{R}_x \int \bar{\boldsymbol{x}}_{\sigma\sigma}(y) + \bar{\boldsymbol{x}}_{\varepsilon\varepsilon}(y) \cdot \mathbb{C}_\varepsilon \, d\Omega(y) + \bar{R}_X \bar{\boldsymbol{X}}_{\sigma\sigma}. \tag{49}$$

Before this set of equations can be solved for $\bar{\boldsymbol{x}}_{\sigma\sigma}$, we must evaluate $\bar{\Omega}_{\sigma\sigma}$. Differentiating (24) and evaluating at $\sigma = 0$ yields

$$\begin{aligned}
\bar{\Omega}_{\sigma\sigma}(y) = &- \int \sum_i \delta\big(z^i - y^i\big) \prod_{j \neq i} \iota\big(z^j - y^j\big) \big(\bar{z}^i_{\sigma\sigma}(z) + \bar{z}^i_{\varepsilon\varepsilon} \cdot \mathbb{C}_\varepsilon\big) \, d\Omega(z) \\
&- \int \sum_i \delta'\big(z^i - y^i\big) \prod_{j \neq i} \iota\big(z^j - y^j\big) \big[\bar{z}^i_\varepsilon(z)\big]^2 \cdot \mathbb{C}_\varepsilon \, d\Omega(z) \\
&+ \int \sum_i \delta\big(z^i - y^i\big) \sum_{j \neq i} \delta\big(z^j - y^j\big) \prod_{k \neq i,j} \iota\big(z^k - y^k\big) \big(\bar{z}^j_\varepsilon(z) \bar{z}^i_\varepsilon(z)\big) \cdot \mathbb{C}_\varepsilon \, d\Omega(z)
\end{aligned}$$

which gives

$$\begin{aligned}
\bar{\omega}_{\sigma\sigma}(y) = &- \sum_i \frac{\partial}{\partial y^i} \big(\big(\bar{z}^i_{\sigma\sigma}(y) + \bar{z}^i_{\varepsilon\varepsilon}(y) \cdot \mathbb{C}_\varepsilon\big) \omega(y) \big) \\
&+ \sum_i \sum_j \frac{\partial^2}{\partial y^i \partial y^j} \big(\big(\bar{z}^i_\varepsilon(y) \bar{z}^j_\varepsilon(y)\big) \cdot \mathbb{C}_\varepsilon \omega(y) \big).
\end{aligned}$$

Following the identical steps as Theorem 1 to show that show that

$$\partial \bar{\boldsymbol{x}}(z) \cdot \bar{\Omega}_{\sigma\sigma} = \mathsf{C}(z) \partial \bar{\boldsymbol{X}} \cdot \bar{\Omega}_{\sigma\sigma} \equiv \mathsf{C}(z) \bar{\boldsymbol{X}}'_{\sigma\sigma}$$

with

$$\begin{aligned}
\bar{\boldsymbol{X}}'_{\sigma\sigma} = &- \left(\bar{R}_x \int \mathsf{C}(y) \, d\Omega(y) + \bar{R}_X \right)^{-1} \bar{R}_x \int \big(\bar{\boldsymbol{x}}_z(y) \mathsf{p}\big(\bar{\boldsymbol{x}}_{\sigma\sigma}(y) + \bar{\boldsymbol{x}}_{\varepsilon\varepsilon}(y) \cdot \mathbb{C}_\varepsilon\big) \\
&+ \bar{\boldsymbol{x}}_{zz}(y) \cdot (\mathsf{p}\bar{\boldsymbol{x}}_\varepsilon, \mathsf{p}\bar{\boldsymbol{x}}_\varepsilon) \cdot \mathbb{C}_\varepsilon \big) \, d\Omega(y).
\end{aligned} \tag{50}$$

We then substitute for $\partial \bar{\boldsymbol{x}} \cdot \bar{\Omega}_{\sigma\sigma} = \mathsf{C}(z) \bar{\boldsymbol{X}}'_{\sigma\sigma}$ in (48) to and solve for $\bar{\boldsymbol{x}}_{\sigma\sigma}(z)$ to find the linear relationship

$$\bar{\boldsymbol{x}}_{\sigma\sigma}(z) = \mathsf{E}_0(z) + \mathsf{E}_1(z) \begin{bmatrix} \bar{\boldsymbol{X}}_{\sigma\sigma} & \bar{\boldsymbol{X}}'_{\sigma\sigma} \end{bmatrix}^\intercal.$$

This relationship can then be plugged into (49) and (50) to yield a linear equation for $\bar{\boldsymbol{X}}_{\sigma\sigma}$ and $\bar{\boldsymbol{X}}'_{\sigma\sigma}$.

A.3. *Expansions in the General Case of Section 3.2*

We extend our method to handle persistent shocks and other endogenous persistent state variables besides the distributional state Ω. To do so, we extend the equilibrium conditions in the following manner:

$$F(\mathbb{E}_- \tilde{\boldsymbol{x}}, \tilde{\boldsymbol{x}}, \mathbb{E}_+ \tilde{\boldsymbol{x}}, \tilde{\boldsymbol{X}}, \Lambda, \boldsymbol{\Theta}, \boldsymbol{\varepsilon}, \boldsymbol{\mathcal{E}}, z) = \mathbf{0}, \tag{51}$$

which must hold for all z in the support of Ω,

$$R\left(\int \tilde{\boldsymbol{x}}\, d\Omega\, d\Pr(\boldsymbol{\varepsilon}), \tilde{\boldsymbol{X}}, \mathbb{E}_+\tilde{\boldsymbol{X}}, \Lambda, \boldsymbol{\Theta}, \boldsymbol{\mathcal{E}}\right) = 0, \tag{52}$$

and a first-order vector autoregression model $\boldsymbol{\Theta}' = \rho_\Theta \boldsymbol{\Theta} + (1-\rho_\Theta)\bar{\boldsymbol{\Theta}} + \boldsymbol{\mathcal{E}}$ for the exogenous shocks. The law of motion of the distribution is given by

$$\widetilde{\Omega}(\Omega, \Lambda, \boldsymbol{\Theta}, \boldsymbol{\mathcal{E}})(z) = \int \iota\big(\tilde{z}(y, \Omega, \Lambda, \boldsymbol{\Theta}, \boldsymbol{\varepsilon}, \boldsymbol{\mathcal{E}}) \le z\big)\, d\Pr(\boldsymbol{\varepsilon})\, d\Omega(y) \quad \forall z. \tag{53}$$

We consider a family of perturbations indexed by a positive scalar σ that scales all shocks $\boldsymbol{\varepsilon}, \boldsymbol{\mathcal{E}}$ so that the policy functions are $\tilde{\boldsymbol{X}}(\Omega, \Lambda, \boldsymbol{\Theta}, \sigma\boldsymbol{\mathcal{E}}; \sigma)$ and $\tilde{\boldsymbol{x}}(z, \Omega, \Lambda, \boldsymbol{\Theta}, \sigma\boldsymbol{\varepsilon}, \sigma\boldsymbol{\mathcal{E}}; \sigma)$. We will use $\bar{\cdot}$ to denote these functions evaluated at $\sigma = 0$.

Unlike Section 3.1, we cannot assume that $\bar{\Omega}(\Omega, \Lambda, \boldsymbol{\Theta})$ is stationary but we recover the independence property.

LEMMA 2: *For any* $\Omega, \Lambda, \boldsymbol{\Theta}$, *the policy functions* $\bar{z}(z, \Omega, \Lambda, \boldsymbol{\Theta})$ *satisfy* $\partial\bar{z}(z, \Omega, \Lambda, \boldsymbol{\Theta}) = \mathbf{0}$ *for all* z *and* $\bar{z}_z(z, \Omega, \Lambda, \boldsymbol{\Theta})$ *independent of* z.

PROOF: We proceed similar to the proof of Lemma 1 in the main text. The first-order condition with respect to $b_{i,t-1}$ yields

$$\mathbb{E}\left[\frac{\big[\tilde{c}(z, \Omega, \Lambda, \boldsymbol{\Theta}, \cdot, \cdot)\big]^{-\nu}}{1 + \tilde{\Pi}(\Omega, \Lambda, \boldsymbol{\Theta}, \cdot,)}\big(\mu - \tilde{\mu}(z, \Omega, \Lambda, \boldsymbol{\Theta}, \cdot, \cdot)\big)\right] = 0.$$

When $\sigma = 0$, this yields $\bar{\mu}(z, \Omega, \Lambda, \boldsymbol{\Theta}) = \mu$ for all z. While equation (20) to the zeroth order is

$$\bar{Q}(\Omega, \Lambda, \boldsymbol{\Theta})\bar{M}(\Omega, \Lambda, \boldsymbol{\Theta})m = \bar{m}(z, \Omega, \Lambda, \boldsymbol{\Theta})\bar{M}\big(\bar{\Omega}(\Omega, \Lambda, \boldsymbol{\Theta})\big)\big(1 + \bar{\Pi}\big(\bar{\Omega}(\Omega, \Lambda, \boldsymbol{\Theta})\big)\big)^{-1}.$$

By construction, the Pareto weights integrate to one, which implies $\bar{m}(z, \Omega, \Lambda, \boldsymbol{\Theta}) = m$ for all z. Finally, the law of motion for θ implies

$$\bar{\boldsymbol{\theta}}(z, \Omega, \Lambda, \Theta) = \rho_\theta \theta.$$

Together they imply $\partial\bar{z}(z, \Omega, \Lambda, \boldsymbol{\Theta}) = \mathbf{0}$ for all z and $\bar{z}_z(z, \Omega, \Lambda, \boldsymbol{\Theta})$ independent of z. *Q.E.D.*

A by product of Lemma 2 is that $\bar{z}_z$ is diagonal. Although we exploit this property in the next section it is not essential.

We start by showing how our expansion extends to the transition path. We assume for a given $\Omega, \Lambda, \boldsymbol{\Theta}$ we have solved for the $\sigma = 0$ transition dynamics $\{\bar{\Omega}^n, \bar{\Lambda}^n, \bar{\boldsymbol{\Theta}}^n\}_{n=0}^N$ with $(\bar{\Omega}^0, \bar{\Lambda}^0, \bar{\boldsymbol{\Theta}}^0) = \Omega, \Lambda, \Theta$ and $(\bar{\Omega}^N, \bar{\Lambda}^N, \bar{\boldsymbol{\Theta}}^N) = (\bar{\boldsymbol{\Omega}}, \bar{\Lambda}, \bar{\boldsymbol{\Theta}})$ at a nonstochastic steady state. Solving the the transition dynamics is eased by the fact that we know, a priori, the transition dynamics of Ω. For the remainder of this Appendix, we use $\bar{\cdot}^n$ to denote derivatives evaluated at $(\bar{\Omega}^n, \bar{\Lambda}^n, \bar{\boldsymbol{\Theta}}^n)$ and, to save on notation, and use $\bar{\cdot}$ to denote derivatives evaluated at the steady state $(\bar{\Omega}^N, \bar{\Lambda}^N, \bar{\boldsymbol{\Theta}}^N)$. We'll start by showing how to compute derivatives at the steady state and then show how to evaluate derivatives along the path.

The policy rules for $\boldsymbol{X}$ and $\boldsymbol{x}$ can then be approximated via Taylor expansion. The first-order expansions for these variables are given by

$$\tilde{\boldsymbol{X}}(\Omega, \Lambda, \boldsymbol{\Theta}, \sigma\boldsymbol{\mathcal{E}}; \sigma) = \bar{\boldsymbol{X}}^0 + \sigma\big(\bar{\boldsymbol{X}}^0_{\boldsymbol{\mathcal{E}}}\boldsymbol{\mathcal{E}} + \bar{\boldsymbol{X}}^0_{\sigma}\big) + \mathcal{O}\big(\sigma^2\big)$$

and

$$\tilde{\boldsymbol{x}}(z, \Omega, \Lambda, \boldsymbol{\Theta}, \sigma\boldsymbol{\varepsilon}, \sigma\boldsymbol{\mathcal{E}}; \sigma) = \bar{\boldsymbol{x}}^0(z) + \sigma\big(\bar{\boldsymbol{x}}^0_{\boldsymbol{\varepsilon}}(z)\boldsymbol{\varepsilon} + \bar{\boldsymbol{x}}^0_{\boldsymbol{\mathcal{E}}}(z)\boldsymbol{\mathcal{E}} + \bar{\boldsymbol{x}}^0_{\sigma}(z)\big) + \mathcal{O}\big(\sigma^2\big).$$

For brevity, we present the necessary derivatives for the first order expansions. Higher-order terms extend analogously to Section A.2.

A.3.1. *Derivatives at the Steady State*

The derivatives of the policy functions with respect to Λ and $\boldsymbol{\Theta}$ as well as the Fréchet derivative with respect to the distribution Ω are used repeatedly in what follows.

Differentiating (51) with respect to Λ yields (Lemma 2 implies that $\bar{\Omega}_\Lambda = 0$).

$$\bar{F}_{x-}(z)\bar{\boldsymbol{x}}_\Lambda(z) + \bar{F}_x(z)\bar{\boldsymbol{x}}_\Lambda(z) + \bar{F}_{x+}(z)\big(\bar{\boldsymbol{x}}_\Lambda(z)\bar{\Lambda}_\Lambda\big) + \bar{F}_X(z)\bar{\boldsymbol{X}}_\Lambda = 0$$

and

$$\bar{R}_x \int \bar{\boldsymbol{x}}_\Lambda(z)\, d\Omega(z) + \bar{R}_X\bar{\boldsymbol{X}}_\Lambda + \bar{R}_{X+}\bar{\boldsymbol{X}}_\Lambda\bar{\Lambda}_\Lambda + \bar{R}_\Lambda = 0.$$

The object $\bar{\Lambda}_\Lambda$is unknown. It requires solving a nonlinear equation, which we show below can be expressed using operations that involve matrices of small dimension. First, note that

$$\bar{\boldsymbol{x}}_\Lambda(z) = -\big(\bar{F}_{x-}(z) + \bar{F}_x(z) + \bar{\Lambda}_\Lambda\bar{F}_{x+}(z)\big)^{-1}\bar{F}_X(z)\bar{\boldsymbol{X}}_\Lambda.$$

Let $\mathsf{A}(z) = -(\bar{F}_{x-}(z) + \bar{F}_x(z) + \bar{\Lambda}_\Lambda\bar{F}_{x+}(z))^{-1}\bar{F}_X(z)$, then

$$\bar{\boldsymbol{X}}_\Lambda = -\left(\bar{R}_x \int \mathsf{A}(z)\, d\Omega(z) + \bar{R}_X + \bar{\Lambda}_\Lambda\bar{R}_{X+}\right)^{-1}\bar{R}_\Lambda.$$

Let P be such that $\Lambda = \mathsf{P}\boldsymbol{X}$. Therefore, $\bar{\Lambda}_\Lambda$ must solve

$$\bar{\Lambda}_\Lambda = -\mathsf{P}\left(\bar{R}_x \int \mathsf{A}(z)\, d\Omega(z) + \bar{R}_X + \bar{\Lambda}_\Lambda\bar{R}_{X+}\right)^{-1}\bar{R}_\Lambda.$$

This can be found easily with a 1-dimensional root solver as all the matrices that need to be inverted are small dimensional.

Next, differentiating (51) with respect to $\boldsymbol{\Theta}$ yields (Lemma 2 implies that $\bar{\Omega}_{\boldsymbol{\Theta}} = 0$).

$$\begin{aligned}&\bar{F}_{x-}(z)\bar{\boldsymbol{x}}_{\boldsymbol{\Theta}}(z) + \bar{F}_x(z)\bar{\boldsymbol{x}}_{\boldsymbol{\Theta}}(z)\\ &\quad + \bar{F}_{x+}(z)\big(\bar{\boldsymbol{x}}_{\boldsymbol{\Theta}}(z)\rho_{\boldsymbol{\Theta}} + \bar{\boldsymbol{x}}_\Lambda(z)\mathsf{P}\bar{\boldsymbol{X}}_{\boldsymbol{\Theta}}\big) + \bar{F}_X(z)\bar{\boldsymbol{X}}_{\boldsymbol{\Theta}} + \bar{F}_{\boldsymbol{\Theta}}(z) = 0.\end{aligned}$$

This yields a linear equation in $\bar{\boldsymbol{x}}_{\boldsymbol{\Theta}}$ and $\bar{\boldsymbol{X}}_{\boldsymbol{\Theta}}$ which we can solve for $\bar{\boldsymbol{x}}_{\boldsymbol{\Theta}}$.[36] Plugging in for the linear relationship between $\bar{\boldsymbol{x}}_{\boldsymbol{\Theta}}$ and $\bar{\boldsymbol{X}}_{\boldsymbol{\Theta}}$ in

$$\bar{R}_x \int \bar{\boldsymbol{x}}_{\boldsymbol{\Theta}}(z)\, d\Omega(z) + \bar{R}_X \bar{\boldsymbol{X}}_{\boldsymbol{\Theta}} + \bar{R}_{X+} \bar{\boldsymbol{X}}_{\boldsymbol{\Theta}} \rho_{\boldsymbol{\Theta}} + \bar{R}_{X+} \bar{\boldsymbol{X}}_{\Lambda} \mathsf{P} \bar{\boldsymbol{X}}_{\boldsymbol{\Theta}} + \bar{R}_{\boldsymbol{\Theta}} = 0,$$

yields a linear equation for $\bar{\boldsymbol{X}}_{\boldsymbol{\Theta}}$.

Finally to determine the Fréchet derivative, we differentiate (51) along the direction Δ. Doing so yields

$$\begin{aligned}\big(\bar{F}_{x-}(z) + \bar{F}_x(z)\big)\partial \bar{\boldsymbol{x}}(z) \cdot \Delta + \bar{F}_{x+}(z) \partial \bar{\boldsymbol{x}}(z) \cdot \partial \bar{\Omega} \cdot \Delta \\ + \bar{F}_{x+}(z) \bar{\boldsymbol{x}}_{\Lambda}(z) \mathsf{P} \partial \bar{\boldsymbol{X}} \cdot \Delta + \bar{F}_X(z) \partial \bar{\boldsymbol{X}} \cdot \Delta = 0.\end{aligned}$$

We first derive an analogue of the property $\partial \bar{\Omega} \cdot \Delta = \Delta$. This holds in the simple Section 3.1 economy but fails in the more general case. We proceed by showing that we can evaluate $\partial \bar{\Omega}$ along a direction Δ^j that satisfies the property that there exists a function $a(\cdot)$ such that the density of Δ^j takes the form

$$\frac{\partial}{\partial \boldsymbol{y}^j}\big(a(\boldsymbol{y}) \bar{\omega}(\boldsymbol{y})\big).$$

Begin by differentiating the law of motion for $\tilde{\Omega}$ at $\sigma = 0$. Since $\partial \bar{\boldsymbol{z}} = 0$, we get

$$\begin{aligned}\big(\partial \bar{\Omega} \cdot \Delta^j\big)(\boldsymbol{y}) &= \int \prod_i \iota\big(\bar{\boldsymbol{z}}^i(z) \le \boldsymbol{y}^i\big) \frac{\partial}{\partial \boldsymbol{z}^j}\big(a(z) \bar{\omega}(z)\big)\, dz \\ &= \int \sum_i \delta\big(\bar{\boldsymbol{z}}^i(z) - \boldsymbol{y}^i\big) \prod_{k \neq i} \iota\big(\bar{\boldsymbol{z}}^k(z) \le \boldsymbol{y}^k\big) \frac{\partial \bar{\boldsymbol{z}}^i}{\partial \boldsymbol{z}^j}(z) a(z) \bar{\omega}(z)\, dz. \\ &= \bar{\boldsymbol{z}}^j_z \int \delta\big(\bar{\boldsymbol{z}}^j - \boldsymbol{y}^j\big) \prod_{k \neq j} \iota\big(\bar{\boldsymbol{z}}^k \le \boldsymbol{y}^k\big) a(z) \bar{\omega}(z)\, dz,\end{aligned}$$

where the second line was achieved through integration by parts. The third line was achieved by noting that $\bar{\omega}$ is the density of the steady state so $\bar{\boldsymbol{z}}(z) = z$ for all z in its support and exploiting that $\frac{\partial \bar{\boldsymbol{z}}^i}{\partial \boldsymbol{z}^j}(z)$ is both independent of z and diagonal. We can also compute the density of $(\partial \bar{\Omega} \cdot \Delta^j)(\boldsymbol{y})$ by applying the derivative $\frac{\partial^{n_z}}{\partial \boldsymbol{y}^1 \partial \boldsymbol{y}^2 \ldots \partial \boldsymbol{y}^{n_z}}$, which gives

$$\bar{\boldsymbol{z}}^j_z \frac{\partial}{\partial \boldsymbol{y}^j} \int \prod_k \boldsymbol{\delta}\big(z^k - \boldsymbol{y}^k\big) a(z) \bar{\omega}(z)\, dz = \bar{\boldsymbol{z}}^j_z \frac{\partial}{\partial \boldsymbol{y}^j}\big(a(\boldsymbol{y}) \bar{\omega}(\boldsymbol{y})\big).$$

We conclude that $\partial \bar{\Omega} \cdot \Delta^j = \bar{\boldsymbol{z}}^j_z \Delta^j$.

Evaluating the Fréchet derivative of (51) in this particular direction Δ^j, we find

$$\begin{aligned}\big(\bar{F}_{x-}(z) + \bar{F}_x(z) + \bar{F}_{x+}(z) \bar{\boldsymbol{x}}_z \mathsf{p} + \boldsymbol{z}^j_z \bar{F}_{x+}(z)\big)\partial \bar{\boldsymbol{x}}(z) \cdot \Delta^j + \bar{F}_{x+}(z) \bar{\boldsymbol{x}}_{\Lambda}(z) \mathsf{P} \partial \bar{\boldsymbol{X}} \cdot \Delta^j \\ + \bar{F}_X(z) \partial \bar{\boldsymbol{X}} \cdot \Delta^j = 0.\end{aligned}$$

[36] Easiest to exploit $\rho_{\boldsymbol{\Theta}} = \left(\begin{smallmatrix} \rho_\Theta & 0 \\ 0 & \rho_\Phi \end{smallmatrix}\right)$ and solve for each column of $\bar{\boldsymbol{x}}_{\boldsymbol{\Theta}}$ separately.

Solving for $\partial\bar{\boldsymbol{x}}(z)\cdot\Delta^j$ we conclude that[37]

$$\begin{aligned}
&\partial\bar{\boldsymbol{x}}(z)\cdot\Delta^j \\
&\quad= -\big(\bar{F}_{x-}(z)+\bar{F}_x(z)+\bar{F}_{x+}(z)\bar{\boldsymbol{x}}_z\mathsf{p}+z_z^j\bar{F}_{x+}(z)\big)^{-1}\big(\bar{F}_{x+}(z)\bar{\boldsymbol{x}}_\Lambda(z)\mathsf{P}+\bar{F}_X(z)\big)\partial\bar{\boldsymbol{X}}\cdot\Delta^j \\
&\quad\equiv \mathsf{C}^j(z)\partial\bar{\boldsymbol{X}}\cdot\Delta^j.
\end{aligned}$$

Taking the derivative of R along this direction, we get

$$\begin{aligned}
\partial\bar{\boldsymbol{X}}\cdot\Delta^j &= -\left(\bar{R}_x\int \mathsf{C}^j(z)\,d\Omega(z)+\bar{R}_{X+}\big(z_z^jI+\bar{\boldsymbol{X}}_\Lambda\mathsf{P}\big)+\bar{R}_X\right)^{-1}\bar{R}_x\int\bar{\boldsymbol{x}}(z)\,d\Delta^j(z) \\
&\equiv \big(\mathsf{D}^j\big)^{-1}\bar{R}_x\int\bar{\boldsymbol{x}}(z)\,d\Delta^j(z).
\end{aligned}$$

From the definition of Δ^j, we can use integration by parts to find that

$$\partial\bar{\boldsymbol{X}}\cdot\Delta^j=\big(\mathsf{D}^j\big)^{-1}\bar{R}_x\int\bar{\boldsymbol{x}}_{z^j}(z)a(z)\,d\Omega(z).$$

A.3.2. *Expansion Along the Path*

We will use the derivatives of the state variables at the end of the transition path to evaluate our expansion along the path using backward induction. This approach is recursive, so we will compute the derivatives at $(\bar{\Omega}^n,\bar{\Lambda}^n,\bar{\boldsymbol{\Theta}}^n)$ assuming derivatives at period $n+1$ of the transition are known.

Differentiating (51) and (52) with respect to Λ, we obtain

$$\bar{F}^n_{x-}(z)\bar{\boldsymbol{x}}^n_\Lambda(z)+\bar{F}^n_x(z)\bar{\boldsymbol{x}}^n_\Lambda(z)+\bar{F}^n_{x+}(z)\bar{\boldsymbol{x}}^{n+1}_\Lambda(z)\mathsf{P}\bar{\boldsymbol{X}}^n_\Lambda+\bar{F}_X(z)\bar{\boldsymbol{X}}^n_\Lambda=0$$

and

$$\bar{R}^n_x\int\bar{\boldsymbol{x}}^n_\Lambda(z)\,d\Omega(z)+\bar{R}^n_X\bar{\boldsymbol{X}}^n_\Lambda+\bar{R}^n_{X+}\bar{\boldsymbol{X}}^{n+1}_\Lambda\mathsf{P}\bar{\boldsymbol{X}}^n_\Lambda+\bar{R}^n_\Lambda=0.$$

As both $\bar{\boldsymbol{x}}^{n+1}_\Lambda(z)$ and $\bar{\boldsymbol{X}}^{n+1}_\Lambda$ are already known, we can solve for $\bar{\boldsymbol{x}}^n_\Lambda(z)$ to find

$$\bar{\boldsymbol{x}}^n_\Lambda(z)=-\big(\bar{\mathsf{F}}^n_{x-}(z)+\bar{\mathsf{F}}^n_x(z)\big)^{-1}\big(\bar{\mathsf{F}}^n_{x+}(z)\bar{\boldsymbol{x}}^{n+1}_\Lambda(z)\mathsf{P}+\bar{\mathsf{F}}^n_X(z)\big)\bar{\boldsymbol{X}}^n_\Lambda,$$

and, therefore, $\bar{\boldsymbol{X}}^n_\Lambda$ equals

$$-\left(-\bar{\mathsf{R}}^n_x\int\big(\bar{\mathsf{F}}^n_{x-}(z)+\bar{\mathsf{F}}^n_x(z)\big)^{-1}\big(\bar{\mathsf{F}}^n_{x+}(z)\bar{\boldsymbol{x}}^{n+1}_\Lambda(z)\mathsf{P}+\bar{\mathsf{F}}^n_X(z)\big)\,d\Omega(z)+\bar{\mathsf{R}}^n_X+\bar{\mathsf{R}}^n_{X+}\bar{\boldsymbol{X}}^{n+1}_\Lambda\mathsf{P}\right)^{-1}\bar{\mathsf{R}}^n_\Lambda.$$

Differentiating with respect to $\boldsymbol{\Theta}$, we find

$$\begin{aligned}
&\bar{F}^n_{x-}(z)\bar{\boldsymbol{x}}^n_{\boldsymbol{\Theta}}(z)+\bar{F}^n_x(z)\bar{\boldsymbol{x}}^n_{\boldsymbol{\Theta}}(z)+\bar{F}^n_{x+}(z)\big(\bar{\boldsymbol{x}}^{n+1}_{\boldsymbol{\Theta}}(z)\rho_{\boldsymbol{\Theta}}+\bar{\boldsymbol{x}}^{n+1}_\Lambda(z)\mathsf{P}\bar{\boldsymbol{X}}^n_{\boldsymbol{\Theta}}\big) \\
&\quad+\bar{F}^n_X(z)\bar{\boldsymbol{X}}^n_{\boldsymbol{\Theta}}+\bar{F}^n_{\boldsymbol{\Theta}}(z)=0.
\end{aligned}$$

[37] For generality, we have written this as one value of C for each individual state, that is, C^j. In fact, one only needs one value for each level of $\bar{z}^j_z$, which in our case is two: 1 and ρ_θ.

This yields a linear equation in $\bar{\boldsymbol{x}}^n_{\boldsymbol{\Theta}}$ and $\bar{\boldsymbol{X}}^n_{\boldsymbol{\Theta}}$, which we can solve for $\bar{\boldsymbol{x}}^n_{\boldsymbol{\Theta}}$ as a linear function of $\bar{\boldsymbol{X}}^n_{\boldsymbol{\Theta}}$. Plugging in for the linear relationship between $\bar{\boldsymbol{x}}^n_{\boldsymbol{\Theta}}$ and $\bar{\boldsymbol{X}}^n_{\boldsymbol{\Theta}}$ in

$$\bar{R}^n_x \int \bar{\boldsymbol{x}}^n_{\boldsymbol{\Theta}}(z)\,d\Omega(z) + \bar{R}^n_X \bar{\boldsymbol{X}}^n_{\boldsymbol{\Theta}} + \bar{R}^n_{X+} \bar{\boldsymbol{X}}^{n+1}_{\boldsymbol{\Theta}} \rho_{\boldsymbol{\Theta}} + \bar{R}_{X+} \bar{\boldsymbol{X}}^{n+1}_{\Lambda} \mathsf{P} \bar{\boldsymbol{X}}^n_{\boldsymbol{\Theta}} + \bar{R}^n_{\boldsymbol{\Theta}} = 0$$

yields a linear equation that can be solved for $\bar{\boldsymbol{X}}^n_{\boldsymbol{\Theta}}$.

To compute the Fréchet derivative, we will evaluate the derivative in direction $\Delta^{j,n}$ with density of the form

$$\frac{\partial}{\partial \boldsymbol{y}^j}\big(a^n(\boldsymbol{y})\bar{\omega}^n(\boldsymbol{y})\big),$$

where $\bar{\omega}^n$ is the density of $\bar{\Omega}^n$ and $a^n(\boldsymbol{y})$ is some arbitrary function. For this derivative, we find

$$\begin{aligned}
\big(\partial\bar{\Omega}^n \cdot \Delta^{j,n}\big)(\boldsymbol{y}) &= \int \prod_i \iota\big(\bar{\boldsymbol{z}}^i(z) \le \boldsymbol{y}^i\big) \frac{\partial}{\partial \boldsymbol{z}^j}\big(a^n(z)\bar{\omega}^n(z)\big)\,dz \\
&= \int \sum_i \delta\big(\bar{\boldsymbol{z}}^i(z) - \boldsymbol{y}^i\big) \prod_{k\neq i} \iota\big(\bar{\boldsymbol{z}}^k(z) \le \boldsymbol{y}^k\big) \frac{\partial \bar{\boldsymbol{z}}^{i,n}}{\partial \boldsymbol{z}^j}(z) a^n(z)\bar{\omega}^n(z)\,dz. \\
&= \bar{\boldsymbol{z}}^j_z \int \delta\big(\bar{\boldsymbol{z}}^i(z) - \boldsymbol{y}^j\big) \prod_{k\neq j} \iota\big(\bar{\boldsymbol{z}}^i(z) \le \boldsymbol{y}^k\big) a^n(z)\bar{\omega}^n(z)\,dz.
\end{aligned}$$

The density of $(\partial\bar{\Omega}^n \cdot \Delta^{j,n})(\boldsymbol{y})$ is found by applying the derivative $\frac{\partial^{n_z}}{\partial \boldsymbol{y}^1 \partial \boldsymbol{y}^2 \cdots \partial \boldsymbol{y}^{n_z}}$ to get

$$\bar{\boldsymbol{z}}^j_z \frac{\partial}{\partial \boldsymbol{y}^j} \int \prod_k \boldsymbol{\delta}\big(\bar{\boldsymbol{z}}^k - \boldsymbol{y}^k\big) a^n(z)\bar{\omega}^n(z)\,dz = \bar{\boldsymbol{z}}^j_z \frac{\partial}{\partial \boldsymbol{y}^j}\big(a^{n+1}(\boldsymbol{y})\bar{\omega}^{n+1}(\boldsymbol{y})\big),$$

where $a^{n+1}(\boldsymbol{y}) = a^n(\bar{\boldsymbol{z}}^{-1}(\boldsymbol{y}))$. We conclude therefore that $\partial\bar{\Omega}^n \cdot \Delta^{j,n} = \bar{\boldsymbol{z}}^j_z \Delta^{j,n+1}$ were we acknowledge the implicit relationship between $\Delta^{j,n}$ and $\Delta^{j,n+1}$ through $a^{n+1}(\boldsymbol{y}) = a^n(\bar{\boldsymbol{z}}^{-1}(\boldsymbol{y}))$.

The Fréchet derivative of F then is

$$\begin{aligned}
&\big(\bar{F}^n_{\boldsymbol{x}-}(z) + \bar{F}^n_{\boldsymbol{x}}(z)\big)\partial\bar{\boldsymbol{x}}^n(z) \cdot \Delta^{j,n} + \boldsymbol{z}^j_z \bar{F}_{x+}(z)\partial\bar{\boldsymbol{x}}^{n+1}(z) \cdot \Delta^{j,n+1} \\
&\quad + \bar{F}^n_{\boldsymbol{x}+}(z)\bar{\boldsymbol{x}}^{n+1}_{\Lambda}(z)\mathsf{P}\partial\bar{\boldsymbol{X}}^n \cdot \Delta^{j,n} + \bar{F}_X(z)\partial\bar{\boldsymbol{X}} \cdot \Delta^{j,n} = 0.
\end{aligned}$$

Since the previous equation is recursive in $\partial\bar{\boldsymbol{x}}^n(z) \cdot \Delta^{j,n}$, we can solve it forward to obtain

$$\partial\bar{\boldsymbol{x}}^n(z) \cdot \Delta^{j,n} = \sum_{k=0}^{N-n} \mathsf{C}^{j,n}_k(z)\partial\bar{\boldsymbol{X}}^{n+k} \cdot \Delta^{j,n+k}$$

with $\mathsf{C}^{j,N}_0$ defined from C^j in the previous section and

$$\begin{aligned}
\mathsf{C}^{j,n}_0(z) &= -\big(\bar{F}^n_{\boldsymbol{x}-}(z) + \bar{F}^n_{\boldsymbol{x}}(z)\big)^{-1}\big(\bar{F}^n_{\boldsymbol{x}+}(z)\bar{\boldsymbol{x}}^{n+1}_{\Lambda}(z)\mathsf{P} + \bar{F}_X(z)\big), \\
\mathsf{C}^{j,n}_k(z) &= -\boldsymbol{z}^j_z\big(\bar{F}^n_{\boldsymbol{x}-}(z) + \bar{F}^n_{\boldsymbol{x}}(z)\big)^{-1}\mathsf{C}^{j,n+1}_{k-1}(z).
\end{aligned}$$

Similarly, differentiating R generates

$$\bar{R}_x^n \int \partial \bar{\boldsymbol{x}}^n(z) \cdot \Delta^{j,n}\, d\Omega^n(z) + z_z^j \bar{R}_{X+}^n \partial \bar{\boldsymbol{X}}^{n+1} \cdot \Delta^{j,n+1} + \bar{\boldsymbol{X}}_\Lambda^{n+1} \mathsf{P} \partial \bar{\boldsymbol{X}}^n \cdot \Delta^{j,n})$$
$$+ \bar{R}_X^n(z) \partial \bar{\boldsymbol{X}}^n \cdot \Delta^{j,n} + \bar{R}_x^n \int \bar{\boldsymbol{x}}^n(z)\, d\Delta^{j,n}(z) = 0.$$

Substituting for $\partial \bar{\boldsymbol{x}}^n(z) \cdot \Delta^{j,n}$ yields a recursive equation with solution

$$\partial \bar{\boldsymbol{X}}^n \cdot \Delta^{j,n} = -\left(\mathsf{D}^{j,n}\right)^{-1} \left(\bar{R}_x^n \int \bar{\boldsymbol{x}}^n(z)\, d\Delta^{j,n} + \sum_{k=1}^{N-n} \mathsf{E}_k^{j,n} \partial \bar{\boldsymbol{X}}^{n+k} \cdot \Delta^{j,n+k} \right)$$

with $\mathsf{D}^{j,N}$ defined by D^j in the previous section and

$$D^{j,n} = \bar{R}_x^n(z) \int \mathsf{C}_0^{j,n}(z)\, d\Omega^n(z) + \bar{R}_{X+}^n \bar{\boldsymbol{X}}_\Lambda^{n+1} \mathsf{P} + \bar{R}_X^n$$

and

$$\mathsf{E}_k^{j,n} = \bar{R}_x^n \int \mathsf{C}_k^{j,n}(z)\, d\Omega^n(z) + \mathbf{1}_{k=1} z_z^j \bar{R}_{X+}^n.$$

Finally, we can use this knowledge to solve for $\bar{\boldsymbol{X}}_\mathcal{E}$. We will give expressions for $\bar{\boldsymbol{X}}_\mathcal{E}^0$ and all others are analogous. Differentiating with respect to $\mathcal{E}$ yields

$$\bar{\mathsf{F}}_x^0(z) \bar{\boldsymbol{x}}_\mathcal{E}^0(z) + \bar{\mathsf{F}}_{x+}^0(z) \big(\bar{\boldsymbol{x}}_\Theta^1(z) + \bar{\boldsymbol{x}}_z^1(z) \mathsf{p} \bar{\boldsymbol{x}}_\mathcal{E}^0(z) + \partial \bar{\boldsymbol{x}}^1(z) \cdot \bar{\Omega}_\mathcal{E}^0 + \bar{\boldsymbol{x}}_\Lambda^1(z) \mathsf{P} \bar{\boldsymbol{X}}_\mathcal{E}^0 \big)$$
$$+ \bar{\mathsf{F}}_X^0(z) \bar{\boldsymbol{X}}_\mathcal{E}^0 + \bar{\mathsf{F}}_\mathcal{E}^0(z) = 0. \tag{54}$$

In order to proceed, we need to determine $\bar{\Omega}_\mathcal{E}^0$. Differentiating the law of motion of Ω gives

$$\bar{\Omega}_\mathcal{E}^0 = -\sum_j \int \delta\big(\bar{z}^j(z) - y^j\big) \prod_i \iota\big(\bar{z}^i(z) \le y^i\big) \bar{z}_\mathcal{E}^{j,0}(z) \bar{\omega}^0(z)\, dz.$$

The density of $\bar{\Omega}_\mathcal{E}^0$ is therefore

$$-\sum_j \frac{\partial}{\partial y^j} \int \prod_i \delta\big(\bar{z}^i(z) - y^i\big) \bar{z}_\mathcal{E}^{j,0}(z) \bar{\omega}^0(z)\, dz = -\sum_j \frac{\partial}{\partial y^j} \big(\bar{z}_\mathcal{E}^{j,0}\big(\bar{z}^{-1}(y)\big) \bar{\omega}^1(y) \big) \equiv \sum_j \bar{\omega}_\mathcal{E}^{0,j,1},$$

where 1 here represents that the objects are evaluated using the density of the transition path at time 1, $\bar{\omega}^1(y)$. If we define $\bar{\Omega}_\mathcal{E}^{0,j,n}$ as the measure with density

$$\bar{\omega}_\mathcal{E}^{0,j,n}(y) = -\frac{\partial}{\partial y^j} \big(\bar{z}_\mathcal{E}^{j,0} \big(\underbrace{\bar{z}^{-1}\big(\cdots \bar{z}^{-1}(y)\big)}_{n \text{ times}} \big) \bar{\omega}^n(y) \big),$$

then

$$\partial \bar{\boldsymbol{x}}^1(z) \cdot \bar{\Omega}_\mathcal{E}^{0,j,1} = \sum_{k=0}^{N-1} \mathsf{C}_k^{j,1}(z) \partial \bar{\boldsymbol{X}}^{1+k} \cdot \bar{\Omega}_\mathcal{E}^{0,j,1+k} \equiv \sum_{k=0}^{N-1} \mathsf{C}_k^{j,1} \bar{\boldsymbol{X}}_\mathcal{E}^{j,1+k}.$$

Combined with (54) gives a linear system

$$\mathsf{M}^0(z)\bar{\boldsymbol{x}}^0_{\boldsymbol{\mathcal{E}}}(z) = \mathsf{N}^0(z)\begin{bmatrix} I & \bar{\boldsymbol{X}}'^{,1,1}_{\boldsymbol{\mathcal{E}}} & \bar{\boldsymbol{X}}'^{,2,1}_{\boldsymbol{\mathcal{E}}} & \cdots & \bar{\boldsymbol{X}}'^{,n_z,N}_{\boldsymbol{\mathcal{E}}} \end{bmatrix}^{\mathsf{T}}$$

and which can be solved for $\bar{\boldsymbol{x}}^0_{\boldsymbol{\mathcal{E}}}(z)$. To find $\bar{\boldsymbol{X}}'^{,j,n}_{\boldsymbol{\mathcal{E}}}$, we note that they satisfy the equation

$$\bar{\boldsymbol{X}}'^{,j,n}_{\boldsymbol{\mathcal{E}}} = -\left(\mathsf{D}^{j,n}\right)^{-1}\left(\bar{R}^n_{z^j} + \bar{R}^n_x \int \left[\bar{\boldsymbol{x}}^n_{z^j}(z)\bar{\boldsymbol{z}}^{j,0}_{\boldsymbol{\mathcal{E}}}(\underbrace{\bar{z}^{-1}(\cdots\bar{z}^{-1}(z))}_{n\text{ times}})\right] d\Omega^n(z) + \sum_{k=1}^{N-n} \mathsf{E}^{j,n}_k \bar{\boldsymbol{X}}'^{,j,n+k}_{\boldsymbol{\mathcal{E}}}\right).$$

Combining the previous equation with

$$\bar{\mathsf{R}}^0_x \int \bar{\boldsymbol{x}}^0_{\boldsymbol{\mathcal{E}}}(z)\, d\Omega^0(z) + \bar{\mathsf{R}}^0_X \bar{\boldsymbol{X}}^0_{\boldsymbol{\mathcal{E}}} + \bar{\mathsf{R}}^0_{X+}\left(\bar{\boldsymbol{X}}^1_{\boldsymbol{\Theta}} + \bar{\boldsymbol{X}}^1_{\boldsymbol{\mathcal{E}}} + \bar{\boldsymbol{X}}^1_{\Lambda}\mathsf{P}\bar{\boldsymbol{X}}^0_{\boldsymbol{\mathcal{E}}}\right) + \bar{\mathsf{R}}^0_{\boldsymbol{\mathcal{E}}} = 0$$

yields a linear system

$$\mathsf{O}\cdot\begin{bmatrix} \bar{\boldsymbol{X}}^0_{\boldsymbol{\mathcal{E}}} & \bar{\boldsymbol{X}}'^{,1,1}_{\boldsymbol{\mathcal{E}}} & \bar{\boldsymbol{X}}'^{,2,1}_{\boldsymbol{\mathcal{E}}} & \cdots & \bar{\boldsymbol{X}}'^{,n_z,N}_{\boldsymbol{\mathcal{E}}} \end{bmatrix}^{\mathsf{T}} = \mathsf{P}$$

which can be solved for $\bar{\boldsymbol{X}}^0_{\boldsymbol{\mathcal{E}}}$.

The term $\bar{\boldsymbol{x}}^0_{\boldsymbol{\varepsilon}}(z)$ satisfies

$$\bar{\boldsymbol{x}}^0_{\boldsymbol{\varepsilon}}(z) = \left(\bar{F}^0_x(z) + \bar{F}^0_{x+}(z)\bar{\boldsymbol{x}}^1_z(\bar{z}(z))\mathsf{p}\right)^{-1}\bar{F}^0_{\boldsymbol{\varepsilon}}(z).$$

A.3.3. *An Alternative Approximation*

In this section, we present the alternative approach highlighted in Section 3.2 where we scale $\{\sigma\boldsymbol{\mathcal{E}}, \sigma\boldsymbol{\varepsilon}, \sigma\boldsymbol{\Theta}, \sigma\theta\}$ and expand with respect to σ instead of just $\{\sigma\boldsymbol{\mathcal{E}}, \sigma\boldsymbol{\varepsilon}\}$.

For this approach, the full policy function for $\boldsymbol{X}$ can be written as $\tilde{\boldsymbol{X}}(\Omega(\sigma), \Lambda, \sigma\boldsymbol{\Theta}, \sigma\boldsymbol{\mathcal{E}}; \sigma)$ where $\Omega(\boldsymbol{y}; \sigma)$ incorporates the fact that we are scaling θ with σ and, therefore, also scaling Ω. Formally, we have (assuming the simplest case where m, μ and θ are the only individual state variables for our problem)

$$\Omega(\mathbf{y}; \sigma) = \int \iota(m \le y_1)\iota(\mu \le y_2)\iota(\sigma\theta \le y_3)\, d\Omega(m, \mu, \theta). \tag{55}$$

The same proof can be used to show that Lemma 2 holds for this approximation as well. There still may be transition dynamics with respect to Λ, at which point it will be necessary to follow Sections A.3.1 and A.3.2 to compute the relevant derivatives for the expansion.[38]

$\tilde{\boldsymbol{X}}$ and $\tilde{\boldsymbol{x}}$ can then be approximated using Taylor expansions with respect to σ. For brevity, we only report the first-order expansion of $\tilde{\boldsymbol{X}}$, which given by

$$\tilde{\boldsymbol{X}}\left(\Omega(\sigma), \Lambda, \sigma\boldsymbol{\Theta}, \sigma\boldsymbol{\mathcal{E}}; \sigma\right) = \bar{\boldsymbol{X}}^0 + \sigma\left(\partial\bar{\boldsymbol{X}}^0 \cdot \bar{\Omega}_\sigma + \bar{\boldsymbol{X}}^0_{\boldsymbol{\Theta}}\boldsymbol{\Theta} + \bar{\boldsymbol{X}}^0_{\boldsymbol{\mathcal{E}}}\boldsymbol{\mathcal{E}} + \bar{\boldsymbol{X}}^0_{\sigma}\right) + \mathcal{O}(\sigma^2).$$

To obtain $\partial\bar{\boldsymbol{X}} \cdot \bar{\Omega}_\sigma$, we differentiate (55) with respect to σ to obtain

$$\bar{\Omega}_\sigma(\mathbf{y}) = -\int \iota(m \le y_1)\iota(\mu \le y_2)\delta(0 - y_3)\theta\, d\Omega(m, \mu, \theta).$$

[38] In the case where there is no endogenous aggregate state variable, only Section A.3.1 is required.

The density of this object is constructed by applying the derivative $\frac{\partial^3}{\partial y_1 \partial y_2 \partial y_3}$ to get

$$\begin{aligned}\bar{\omega}_\sigma(\mathbf{y}) &= -\frac{\partial}{\partial y_3}\left(\int \delta(m-y_1)\delta(\mu-y_2)\delta(0-y_3)\theta\, d\Omega(m,\mu,\theta)\right)\\ &= -\frac{\partial}{\partial y_3}\left(\delta(0-y_3)\int \omega(y_1,y_2,\theta)\theta\, d\theta\right)\\ &= -\frac{\partial}{\partial y_3}\big(E\theta(y_1,y_2)\bar{\omega}(\mathbf{y})\big),\end{aligned}$$

where in the last equality we defined $E\theta(y_1,y_2) = \frac{\int \omega(y_1,y_2,\theta)\theta\, d\theta}{\int \omega(y_1,y_2,\theta)\, d\theta}$ as the cross-sectional mean of θ conditional on $(m,\mu) = (y_1, y_2)$. From this expression, we know that $\partial \bar{\boldsymbol{X}}^0 \cdot \bar{\Omega}_\sigma$ can be solved for in the same manner as $\partial \bar{\boldsymbol{X}}^0 \cdot \bar{\Omega}^0_{\boldsymbol{\varepsilon}}$ using the tools in Section (A.3.2).

A.3.4. *Simulation and Clustering*

To simulate an optimal policy at each date with N agents, we discretize the distribution across agents with K grid points that we find each period using a k-means clustering algorithm. Let $\{z_i\}_{i=1}^N$ represent the current distribution of agents. The k-means algorithm generates K points $\{\bar{z}_k\}_{k=1}^K$ with each agent i assigned to a cluster $k(i)$ to minimize the squared error $\sum_i \|z_i - \bar{z}_{k(i)}\|^2$. We let Ω represent the distribution of N agents and $\bar{\Omega}$ represent our approximating distribution of clusters.[39] At each history, we compute $\bar{\Omega}$ and then apply our algorithm to approximate the optimal policies around $\bar{\Omega}$.[40] When $K = N$, we exactly approximate around Ω, but for $K < N$ we can speed up the computations by a factor of $\frac{N}{K}$.

A.3.5. *Solving the $t = 0$ Problem*

For the Ramsey problem (21), optimality conditions at $t = 0$ are different from $t \geq 1$. The full set of optimality conditions are represented by expanding equations (22)–(24). We describe how to apply our procedure for the Section 3.1 simple case. The extension to the general problem in Section 2 is straightforward. We outline two ways to solve the $t = 0$ problem below. Both the methods have the same degree of approximation errors for impulse responses but they would differ for other simulations of Ramsey allocation.

We start with some notation for the first method. Let Ω^B be a measure over the claims to risk-free debt. Denote the $t = 0$ aggregate policy functions as $\tilde{\boldsymbol{X}}_0(\Omega^B, \boldsymbol{\mathcal{E}}_0)$ and individual policy functions as $\tilde{\boldsymbol{x}}_0(b, \Omega^B, \boldsymbol{\varepsilon}_0, \boldsymbol{\mathcal{E}}_0)$. Augment the system (22)–(24) with mappings F_0 and R_0, capturing the time 0 first-order conditions, such that

$$F_0(\tilde{\boldsymbol{x}}_0, \mathbb{E}_+\tilde{\boldsymbol{x}}, \tilde{\boldsymbol{X}}_0, \boldsymbol{\varepsilon}_0, \boldsymbol{\mathcal{E}}_0, b_0) = \mathbf{0}, \tag{56}$$

$$R_0\left(\int \tilde{\boldsymbol{x}}_0\, d\Omega^B, \tilde{\boldsymbol{X}}_0, \boldsymbol{\mathcal{E}}_0\right) = \mathbf{0}. \tag{57}$$

[39] Formally, $\Omega(z)$ has density $\sum_i \frac{1}{N}\delta(z - z_i)$ while $\bar{\Omega}(z)$ has density $\sum_i \frac{1}{N}\delta(z - \bar{z}_{k(i)})$.

[40] Similar to Section (A.3.3), this is done by constructing a distribution $\bar{\Omega}(\sigma)$ with density $\sum_i \frac{1}{N}\delta(z - \bar{z}_{k(i)} - \sigma(z_i - \bar{z}_{k(i)}))$ and then computing $\partial \bar{\boldsymbol{X}}^0 \cdot \bar{\Omega}_\sigma$ in the same manner as Section (A.3.3).

Policy functions for $t \geq 1$ individual states $z_0 = (m_0, \mu_0)$ are components of $\tilde{\boldsymbol{x}}_0$. Let function $\Omega_0(\Omega^B, \boldsymbol{\mathcal{E}}_0)$ map the initial condition Ω^B and aggregate shock $\boldsymbol{\mathcal{E}}_0$ to a measure Ω over z using

$$\Omega_0\big(\Omega^B, \boldsymbol{\mathcal{E}}_0\big)(z) = \int \iota\big(\tilde{z}_0\big(y, \Omega^B, \boldsymbol{\varepsilon}_0, \boldsymbol{\mathcal{E}}_0\big) \leq z\big)\, d\Pr(\boldsymbol{\varepsilon}_0)\, d\Omega^B(y) \quad \forall z. \tag{58}$$

Section 3.1 characterizes the small-noise approximations of the $t \geq 1$ policy functions around an arbitrary Ω. We update Ω along the path by iterating between an approximation and a simulation step. At some $t \geq 1$, taking as input Ω_{t-1}, we draw idiosyncratic shocks $\boldsymbol{\varepsilon}$ for each agent as well as aggregate shocks $\boldsymbol{\mathcal{E}}$, and use the policy functions approximated around Ω_{t-1} to move to the next period Ω_t. All that remains to be specified is how the $t = 1$ state, Ω_0, is obtained. We do that below by constructing small-noise approximations to $t = 0$ policy functions: $\tilde{\boldsymbol{X}}_0(\Omega^B, \sigma\boldsymbol{\mathcal{E}}_0; \sigma)$ and $\tilde{\boldsymbol{x}}_0(b, \Omega^B, \sigma\boldsymbol{\varepsilon}_0, \sigma\boldsymbol{\mathcal{E}}_0; \sigma)$. We present a first- order expansion. Higher-order expansions along the lines of Section A.2 are analogous.

1. Zeroth order: For some choice of Ω^B, the $\sigma = 0$ allocation consists of $\{\bar{\boldsymbol{x}}_0(b), \bar{\boldsymbol{x}}(b)\}$ for b in support of Ω^B as well as $\{\bar{\boldsymbol{X}}_0, \bar{\boldsymbol{X}}\}$ such that

$$F_0(\bar{\boldsymbol{x}}_0, \bar{\boldsymbol{x}}, \bar{\boldsymbol{X}}_0, 0, 0, b_0) = \boldsymbol{0}, \qquad R_0\left(\int \bar{\boldsymbol{x}}_0(b)\, d\Omega^B(b), \bar{\boldsymbol{X}}_0, \boldsymbol{\mathcal{E}}_0\right) = \boldsymbol{0},$$

$$F(\bar{\boldsymbol{x}}, \bar{\boldsymbol{x}}, \bar{\boldsymbol{x}}, \bar{\boldsymbol{X}}, 0, 0, \bar{z}) = \boldsymbol{0}, \qquad R\left(\int \bar{\boldsymbol{x}}(b)\, d\Omega^B(b), \bar{\boldsymbol{X}}, 0\right) = \boldsymbol{0}.$$

2. To compute derivatives $\{\bar{\boldsymbol{x}}_{0,\varepsilon}(b), \bar{\boldsymbol{x}}_{0,\boldsymbol{\mathcal{E}}}(b), \bar{\boldsymbol{x}}_{0,\sigma}(b), \bar{\boldsymbol{X}}_{0,\boldsymbol{\mathcal{E}}}, \bar{\boldsymbol{X}}_{0,\sigma}\}$, we use the formulas from Section A.3.2. The expressions that appear in Section A.3.2 use superscript n to denote the period of transition path for the $\sigma = 0$ allocation. We can obtain $\{\bar{\boldsymbol{x}}_{0,\varepsilon}(b), \bar{\boldsymbol{x}}_{0,\boldsymbol{\mathcal{E}}}(\boldsymbol{b}), \bar{\boldsymbol{x}}_{0,\sigma}(b), \bar{\boldsymbol{X}}_{0,\boldsymbol{\mathcal{E}}}, \bar{\boldsymbol{X}}_{0,\sigma}\}$ by using those formulas after replacing $F^0_\bullet$ with $F_{0,\bullet}$, $F^n_\bullet$ with $F_\bullet$ for $n \geq 1$ and similarly for $R^0_\bullet$ and $R^n_\bullet$.
3. Simulation: Draw idiosyncratic shocks $\boldsymbol{\varepsilon}_0$ for each agent as well as aggregate shocks $\boldsymbol{\mathcal{E}}_0$ and use the approximations to policy functions

$$\tilde{\boldsymbol{X}}_0\big(\Omega^B, \sigma\boldsymbol{\mathcal{E}}_0; \sigma\big) = \bar{\boldsymbol{X}}_0 + \sigma\big(\bar{\boldsymbol{X}}_{0,\boldsymbol{\mathcal{E}}}\boldsymbol{\mathcal{E}}_0 + \bar{\boldsymbol{X}}_{0,\sigma}\big) + \mathcal{O}\big(\sigma^2\big)$$

and

$$\tilde{\boldsymbol{x}}\big(b, \Omega^B, \sigma\boldsymbol{\varepsilon}_0, \sigma\boldsymbol{\mathcal{E}}_0; \sigma\big) = \bar{\boldsymbol{x}}_0(b) + \sigma\big(\bar{\boldsymbol{x}}_{0,\varepsilon}(b)\boldsymbol{\varepsilon}_0 + \bar{\boldsymbol{x}}_{0,\boldsymbol{\mathcal{E}}}(b)\boldsymbol{\mathcal{E}}_0 + \bar{\boldsymbol{x}}_{0,\sigma}(b)\big) + \mathcal{O}\big(\sigma^2\big)$$

to obtain the $\Omega_0(z_0)$ for $t = 1$.

We now describe the second method. The second method is quicker to implement and provides equally accurate (as compared to the first method) approximations as far as impulse responses of the Ramsey allocation are concerned. Define $\bar{\Omega}_0$ as the state chosen by a Ramsey planner when $\sigma = 0$ for some initial condition Ω^B. The $\sigma = 0$ problem is easy to solve because the optimal allocation is stationary. This follows from the feature that $t = 0$ the planner can set all fiscal instruments, $\Upsilon = (\Upsilon^n, \Upsilon^d, \Upsilon^b)$ and in absence of shocks does not need to reoptimize. One can show that $\Omega_0 = \bar{\Omega}_0 + \mathcal{O}(\sigma^2)$ and, therefore, impulse response functions replacing Ω_0 with $\bar{\Omega}_0$ agree up to order $\mathcal{O}(\sigma^3)$. We use the second method to compute impulse responses in the main text.

A.4. *Additional Details for Section 3.3*

In this section, we provide more details concerning Acharya and Dogra (2018) "PRANK" economy, which we use as a laboratory to test the accuracy of our algorithm and compare it to alternative methods. We start with equilibrium conditions, next we discuss the calibration, and report the accuracy tests for our method. Finally, we present a simplified version of this economy for which we can solve for all gradients in closed form.

A.4.0.1. *Equilibrium in the PRANK Economy.* To obtain the PRANK setting, we impose the following assumptions: (i) labor is supplied inelastically, and period utility function $U(c_t, n_t) = -\exp(-\gamma c_t)$, (ii) the distribution of shares is uniform, (iii) idiosyncratic productivity shocks are i.i.d, and (iv) all tax rates are constant and the monetary policy follows a Taylor rule given by

$$Q_t^{-1} - 1 = a_0(1 + \Pi_t)^{a_1}. \tag{59}$$

In the PRANK economy, a perfect foresight equilibrium is constructed as follows. For a sequence of innovations to TFP $\{\mathcal{E}_{\Theta,s}\}_{s=0}^{T}$, Agent is consumption $c_{i,t}$ satisfies

$$c_{i,t} = \mathcal{C}_t + \mu_t\left(\frac{b_{i,t-1}}{1+\Pi_t} + y_{i,t}\right), \tag{60}$$

where $y_{i,t} = (1 - \Upsilon_t)W_t\epsilon_{i,t}n_{i,t} + T_t + d_{i,t}$ is the households income at date t. The two parameters $\mathcal{C}_t$ and μ_t that are common to all agents are given by

$$\mu_t = \frac{\mu_{t+1}\left(\frac{Q_t}{1+\Pi_{t+1}}\right)}{1 + \mu_{t+1}\left(\frac{Q_t}{1+\Pi_{t+1}}\right)}, \tag{61}$$

$$\mathcal{C}_t\left[1 + \mu_{t+1}\left(\frac{Q_t}{1+\Pi_{t+1}}\right)\right] = -\frac{1}{\gamma}\ln\beta\left(\frac{Q_t}{1+\Pi_{t+1}}\right) + \mathcal{C}_{t+1} + \mu_{t+1}\bar{y}_{t+1} - \frac{\gamma\mu_{t+1}^2\sigma_{y,t+1}^2}{2}, \tag{62}$$

where $\bar{y}_{t+1} = \int y_{i,t+1}\,di$ is the average household income, and $\sigma_{y,t+1}^2$ is the variance in household level income. A perfect foresight equilibrium can by solving equations (59)–(62) along with equations (8), (10), (16), and (17).

We check the accuracy of our approximations using an exact solution to the perfect foresight equilibrium. Section A.4.0.2 discusses how we calibrate the PRANK economy, Sections A.4.0.3 and A.4.0.4 compare approximation errors using several diagnostics.

A.4.0.2. *Calibration.* We study several cases. For the parameters that are common across these cases, we use Acharya and Dogra (2018) targets, which are are quite standard in the representative agent New Keynesian literature. The discount rate β to 0.96 to get a real rate of 4% per year, the elasticity of substitution parameter, Φ, to 6 to target an average markup of 20%. The share of intermediate inputs α is set to 0.6 to target a labor income share of 2/3, and we set the adjustment cost parameter ψ to 41.6 to target a slope of the Phillips curve of 0.06. Aggregate productivity follows an AR(1) process with a decay parameter 0.73, and the standard deviation of the innovation is set to 1.23% to be consistent with de trended output per hour and we turn off the markup shocks. For the Taylor rule parameters, we set $a_1 = 1.5$ and choose a_0 to target 0% inflation rate

in absence of aggregate risk. We vary the standard deviation of idiosyncratic risk, $\sigma_\epsilon \in \{0.5, 0.75, 1\}$, and the risk aversion parameter, $\gamma \in \{1, 3\}$. Our calibrations cover a range that includes Acharya and Dogra (2018) as well as what we use in our baseline Section 4. Since the distribution of assets is nonstationary, we set $\Omega_0(b)$ to be Gaussian and calibrate the parameters to be consistent with the distribution of wealth in the SCF. For simulation, we approximate the distribution with 150 points and the idiosyncratic shocks with 10-point Gaussian quadrature.

A.4.0.3. *Diagnostics.* In this section, we compare the accuracy of our policy functions in two settings. We start with a stationary environment with no aggregate risk and study the policy function for individual consumption as well as values for the aggregate variables. Then we study impulse responses of several aggregate variables to a TFP shock. As mentioned before, the advantage of PRANK is that in both cases, the true solution can be solved exactly.

We report three types of approximation errors for the individual policy functions that are defined in the main text. For all of the experiments, we use a second-order approximation of our method. As a point of comparison, we report the errors when policy functions are approximated using the Reiter-approach (also used in Acharya and Dogra (2018)) in which the no-aggregate risk economy is solved exactly, and then the policy functions are linearized with respect to aggregate shocks. In all our plots, our method will be represented by a bold blue line, the Reiter approximation will be represented by a dashed black line and the exact solution will be a bold black line.

We begin with the approximation errors turning off aggregate risk. By construction, the errors for the Retier-method are zero and so we report the error diagnostics just for our method for several values of $\{\sigma_\epsilon, \gamma\}$ in Table V. The maximum percent errors in the individual policy rules for consumption relative to the exact solution are small starting at 0.0039% for our baseline calibration and raising to only 0.0328% when we double the size of the idiosyncratic risk. The Euler equation errors are comparable. We see a similar pattern in the errors for the aggregate variables, though the errors for those are an order of magnitude smaller.

Next, we compare the errors in the policy functions in response to an one time one standard deviation unanticipated shock to aggregate productivity. We report these errors in Table VI. For the individual consumption policy functions, the maximum errors (across the state space (b, ϵ) and across time t) for our second-order approach are comparable to the Reiter method. In fact, while the Euler equation errors $E^{\text{EE}}_{c,t}(b, \epsilon)$ for the Reiter method are generally smaller than our second-order approximation, the errors relative to

TABLE V

APPROXIMATION ERRORS—NO AGGREGATE RISK.

	Individual Consumption					
Maximum Errors (%)	Policy	Euler	Dyn. Euler	Agg. Output	Inflation	Interest Rate
$\gamma = 1$, $\sigma_\epsilon = 0.5$	0.0039	0.0031	0.0097	5.2e−6	3.1e−5	4.3e−5
$\gamma = 1$, $\sigma_\epsilon = 0.75$	0.0134	0.0105	0.0207	2.6e−5	1.6e−4	2.2e−4
$\gamma = 1$, $\sigma_\epsilon = 1.0$	0.0328	0.0249	0.0705	4.9e−4	6.9e−4	8.2e−4
$\gamma = 3$, $\sigma_\epsilon = 0.5$	0.0453	0.0280	0.1220	4.1e−4	2.4e−3	3.4e−3

Note: Percentage errors in policy functions with no aggregate risk. The values reported are the maximum errors across the state space (b, ϵ). The columns "Policy," "Euler," and "Dyn. Euler" refer to the diagnostic measure $E^{\text{pol}}_{c,t}(b, \epsilon)$, $E^{\text{EE}}_{c,t}(b, \epsilon)$, and $E^{\text{dynEE}}_{c,t}(b, \epsilon)$, respectively.

TABLE VI

APPROXIMATION ERRORS—AGGREGATE RISK.

	Individual Consumption					
Maximum Errors (%)	Policy	Euler	Dyn. Euler	Agg. Output	Inflation	Interest Rate
			2nd Order			
$\gamma = 1$, $\sigma_\epsilon = 0.50$	0.0039	0.0031	0.0103	4.2e−6	3.1e−5	4.3e−5
$\gamma = 1$, $\sigma_\epsilon = 0.75$	0.0134	0.0105	0.0402	2.6e−5	1.5e−4	2.2e−4
$\gamma = 1$, $\sigma_\epsilon = 1.00$	0.0328	0.0249	0.0853	8.2e−5	4.9e−4	6.9e−4
$\gamma = 3$, $\sigma_\epsilon = 0.5$	0.0453	0.0280	0.1091	0.0011	0.0024	0.0034
			Reiter-Based			
$\gamma = 1$, $\sigma_\epsilon = 0.50$	0.0374	0.0022	0.0153	0.0616	0.0337	0.0505
$\gamma = 1$, $\sigma_\epsilon = 0.75$	0.0466	0.0022	0.0208	0.0610	0.0335	0.0501
$\gamma = 1$, $\sigma_\epsilon = 1.00$	0.0492	0.0023	0.0364	0.0602	0.0329	0.0493
$\gamma = 3$, $\sigma_\epsilon = 0.5$	0.0896	0.0038	0.0462	0.2252	0.1327	0.1991

Note: Percentage errors in policy functions in response to an one standard deviation unanticipated shock to aggregate TFP. The values reported are the maximum errors across states (b, ϵ) and time t. The columns "Policy," "Euler," and "Dyn. Euler" refer to the diagnostic measure $E^{\text{pol}}_{c,t}(b,\epsilon)$, $E^{\text{EE}}_{c,t}(b,\epsilon)$, and $E^{\text{dynEE}}_{c,t}(b,\epsilon)$, respectively.

the exact solution $E^{\text{pol}}_{c,t}(b,\epsilon)$ are an order of magnitude larger (0.0039% vs. 0.0404%). The diagnostic errors $E^{\text{pol}}_{c,t}(b,\epsilon)$ clearly captures errors coming from aggregate shocks that are not reflected in the Euler equation errors. We also see that the dynamic Euler equation errors remain small and comparable to those of the Reiter approach, which indicates that one should not be too concerned with errors accumulating over time.

Tables V and VI also report errors for the alternative calibrations where we increase risk aversion, γ, to 3. Not surprisingly increasing risk aversion leads to the largest policy errors for both our second-order approximation as well as the Retier methods, but the policy errors remain small and are comparable to those from the Reiter approach. Figure 10 reproduces the impulse responses in Figure 1 of the main text for $\gamma = 3$. For larger values

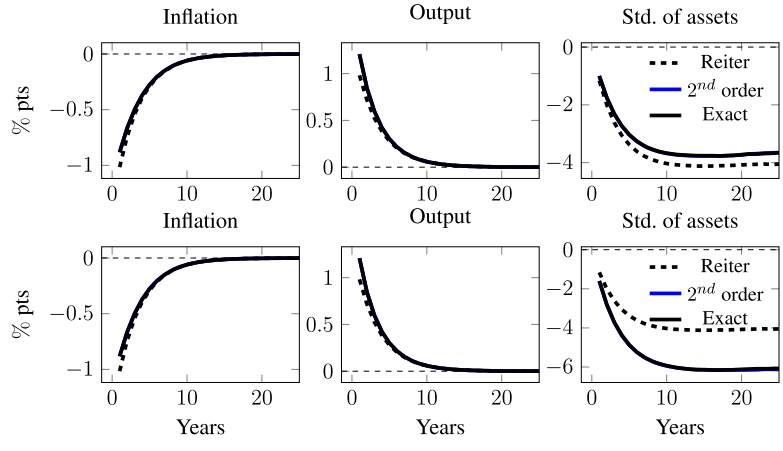

FIGURE 10.—Comparisons for impulse responses to a 1% TFP shock at $t = 1$ in the top panel and $t = 250$ in the bottom panel.

of risk aversion, we see a visible deviation of the Reiter approach from both the exact solution and our second-order approximations. The visible deviation reflects the errors in aggregates of the Reiter approach documented in Table VI.

A.4.0.4. *Long Run Errors.* In the PRANK economy, individual assets follow an approximate random walk and, therefore, the distribution of individual savings drifts over time. Since our method approximates with respect to the size of idiosyncratic risk, a diagnostic for whether small errors at a point in time accumulate to large error over time, we check how well the approximated distribution of assets tracks the true distribution with our method as well as with the Reiter method.

In Figure 11, we plot the distribution of assets obtained at $t = 250$ after a one-standard deviation shock at $t = 0$. We see the second-order approximation lines up very closely with the Reiter method and to the outcomes from the exact solution. This figure also explains the finding in Section 3.3, why our method captures the the response of inequality to an unanticipated TFP shock $t = 250$ so well.

We next compare the distribution of assets after a sequence of TFP shocks in a stochastic PRANK economy. The TFP shocks follow an AR(1) and for this exercise we do not have the true solution in an analytic form. However, we can still compare our second-order approximation and the Reiter approach. In addition, we include a "hybrid" method where we take a second-order approximation with respect to idiosyncratic shocks and a first-order approximation with respect to aggregate shocks.

In Figure 12, we see that the hybrid and Reiter approaches produce nearly identical distributions after these shocks, but the second-order approach delivers a tighter distribution over time. As the hybrid approach was obtained by dropping the second-order terms with respect to aggregate shocks, we take this as evidence that, in this model, ignoring those second-order terms can lead long run drift away from the true solution.

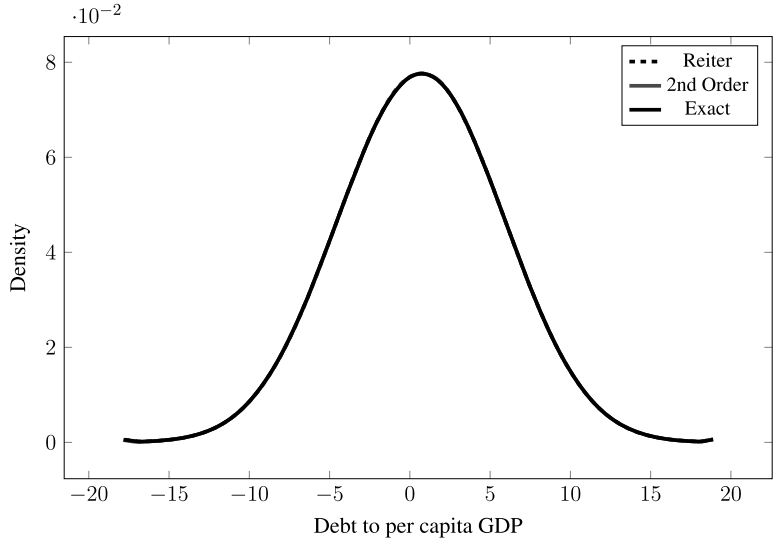

FIGURE 11.—Distribution of assets at $t = 250$ following a one-time unanticipated TFP shock at $t = 0$.

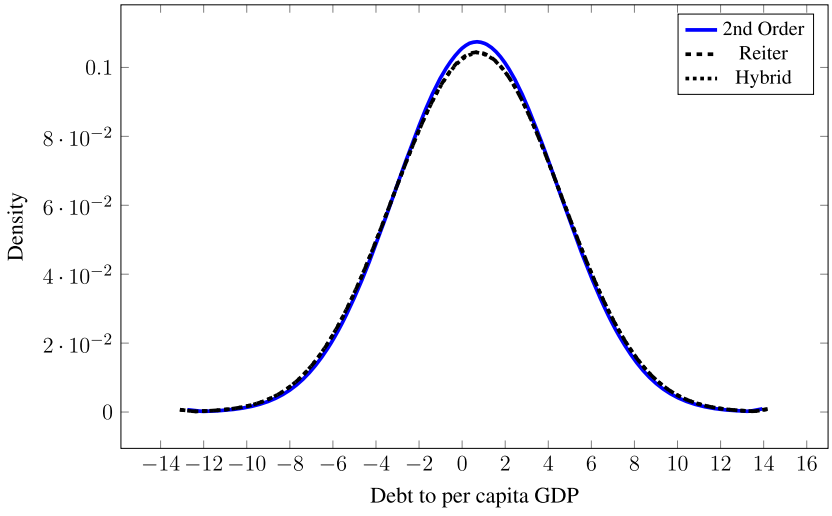

FIGURE 12.—Distribution of assets $t = 250$ in the stochastic PRANK economy after a sequence of TFP shocks.

A.4.0.5. *A Simplified Example.* To illustrate how our approach from Section 3 is applied to the PRANK economy, we present a version of the PRANK economy where we can explicitly show how to compute all the gradients that appear that section. We assume aggressive enough monetary policy to ensure $\Pi_t = 0$ for all t; that share of intermediate inputs, $1 - \alpha$, is 0, which ensures that output is linearly related to productivity; and finally that $\Phi \to \infty$ to ensure that there are no markups and dividends. The environment is similar to the well-known Huggett (1993) model and can be trivially solved with standard methods; we use it to illustrate transparently how to construct all the objects that appear in Section 3.

The economy is populated with a continuum of infinitely lived consumers who receive endowment shocks. Let $e_{i,t}$ be endowment of consumer i in period t. Endowments are subject to aggregate shock $\mathcal{E}_t$ and idiosyncratic shock $\varepsilon_{i,t}$ and satisfy

$$e_{i,t} = 1 + \varepsilon_{i,t} + \mathcal{E}_t.$$

Shocks $\mathcal{E}_t$ and $\varepsilon_{i,t}$ are mean zero and i.i.d. over time.

Competitive equilibrium in this economy is fully characterized by consumer budget constraint and the Euler equation

$$c_{i,t} + Q_t b_{i,t} - 1 - \varepsilon_{i,t} - \mathcal{E}_t - b_{i,t-1} = 0,$$
$$Q_t \exp(-\gamma c_{i,t}) - \beta \mathbb{E}_{i,t} \exp(-\gamma c_{i,t}) = 0$$

as well as the feasibility

$$\int c_{i,t}\, di - 1 - \mathcal{E}_t = 0.$$

We now show how to use our approximation techniques in this simple example to find competitive equilibrium. To make it similar to our notation in Section 3, let $y = \exp(-\gamma c)$ and rewrite this problem as

$$c_{i,t} + Q_t b_{i,t} - 1 - \varepsilon_{i,t} - \mathcal{E}_t - b_{i,t-1} = 0,$$

$$Q_t y_{i,t} - \beta \mathbb{E}_{i,t} y_{i,t+1} = 0,$$
$$y_{i,t} - \exp(-\gamma c_{i,t}) = 0.$$

The first pair of equations correspond to (22) and define mapping F, the last equation corresponds to (23) and define R. This problem is recursive in the distribution of agents' assets. In our notation of Section 3, we have $z = b$ and Ω is the distribution of b such that $\int b \, d\Omega = 0$. Vector $\tilde{\boldsymbol{x}}$ of individual policy functions is given by three policy functions $[\tilde{b} \;\; \tilde{c} \;\; \tilde{y}]^{\mathrm{T}}$, and $\tilde{Q}$ is the only aggregate policy function in vector $\boldsymbol{X}$. Selection matrix p is simply $[1 \;\; 0 \;\; 0]$.

It is immediate to verify that without shocks consumption smoothing implies that $\bar{b}(b) = b$ for all b, so that Lemma 1 holds and equation (27) becomes

$$\bar{c}(b) + \bar{Q}\bar{b}(b) - 1 - b = 0,$$
$$\bar{Q}\bar{y}(b) - \beta \bar{y}\big(\bar{b}(b)\big) = 0,$$
$$\bar{y}(b) - \exp\big(-\gamma \bar{c}(b)\big) = 0$$

and

$$\int \bar{c}(b) \, d\Omega - 1 = 0,$$

which immediately gives $\bar{Q} = \beta$ and $\bar{c}(b) = 1 + (1-\beta)b$, $\bar{y}(b) = \exp(-\gamma \bar{c}(b))$. From these, we construct mappings $\mathsf{R}_x = [1\,0\,0]$, $\mathsf{R}_X = 0$, $\mathsf{R}_{\boldsymbol{\varepsilon}} = -1$, and $\mathsf{F}_{x-}(b) = \mathbf{0}$,

$$\mathsf{F}_x(b) = \begin{bmatrix} \bar{Q} & 1 & 0 \\ 0 & 0 & \bar{Q} \\ 0 & -\gamma \exp\big(-\gamma \bar{c}(b)\big) & 1 \end{bmatrix}, \qquad \mathsf{F}_{x+}(b) = \begin{bmatrix} 0 & 0 & 0 \\ 0 & 0 & -\beta \\ 0 & 0 & 0 \end{bmatrix},$$

$$\mathsf{F}_X(b) = \begin{bmatrix} b \\ \bar{y}(b) \\ 0 \end{bmatrix}, \qquad \mathsf{F}_{\varepsilon}(b) = \begin{bmatrix} -1 \\ 0 \\ 0 \end{bmatrix}, \qquad \mathsf{F}_{\boldsymbol{\varepsilon}}(b) = \begin{bmatrix} -1 \\ 0 \\ 0 \end{bmatrix}, \qquad \mathsf{F}_z(z) = \begin{bmatrix} -1 \\ 0 \\ 0 \end{bmatrix}.$$

All elements of these matrices are know from the zeroth-order expansion. Using them, we construct first-order approximations of policy functions as described in the text.

APPENDIX B: ADDITIONAL DETAILS FOR SECTION 4

In this section, we provide details of how we calibrate the initial distribution of nominal and real claims using the Doepke and Schneider (2006) procedure. Then we show the dynamics of the calibrated competitive equilibrium using simulations.

Initial Distribution of Nominal and Real Claims. We combine the rich house-level data on financial assets from the Survey of Consumer Finances (SCF) and the aggregated Flow of Funds for intermediate investors to obtain nominal and real exposures. We start with the 2007 Wave of the SCF and restrict our sample to married households who work at least 100 hours. We drop observations where equity or bond holdings are more than 100 times the average yearly wage. These turned out to be about 0.5% of the total sample. We extract household-level data on their financial holdings and categorize them into (i) deposits, government bonds, liquid assets (net of unsecured credit), (ii) direct holdings of

claims to corporate equities and corporate bonds, and (iii) indirect holdings of (i) and (ii) through mutual funds and retirement accounts.

We then use Flow of Funds data to obtain balance sheet information for private pensions (Table L.118), for state and local pensions (Table L.119) and mutual funds (Table L.122). Since pension funds have a nontrivial exposure to mutual funds and not vice versa, we start with the aggregated mutual fund balance sheet and map it into broad categories that represent deposits, corporate bonds, government bonds, corporate equities. In the year 2007, mutual funds invested 84% of their assets in corporate equities and bonds, 16% in government bonds and other liquid claims.

We next turn pension funds and after aggregating private and public pension funds categorize the combined assets into deposits, government-issued debt, corporate debt, corporate equities, and mutual funds. For the year 2007, the pension funds assets were invested 22% in mutual funds, 63% in corporate equities and bonds, and the rest being 15% in government bonds and other liquid claims.

We define nominal claims as money-like assets plus government issued bonds and claims to real profits as corporate bonds plus corporate equities. Using the information above, we first consolidate the mutual funds into these two categories and then reassign the mutual funds to pension funds, and finally the mutual funds and pensions funds to the individuals in the SCF.

To fit initial states, we sample directly from the SCF log wages, nominal claims, and claims to real profits that we constructed. The SCF provides population weights for each observation. Given these weights, we set the initial condition by drawing with replacement a random sample of 100,000 agents from a discrete distribution.

Properties of the Competitive Equilibrium. In this section, we report several moments from our calibrated competitive equilibrium along a transition path. We draw a sequence of markup and TFP shocks of length 100 and simulate the competitive equilibrium policies using 100,000 agents. When we simulate the competitive equilibria, we keep the tax rates $\Upsilon_t = \bar{\Upsilon}$ and use a Taylor rule with $Q_t^{-1} = \frac{1}{\beta}\Pi_t^{2.5}$.

In Figure 13, we plot the time series for aggregate output and labor share. We see that the aggregates are quite stationary and exhibit small fluctuations due to productivity and markup shocks. In Table VII, we report cross-sectional moments at dates

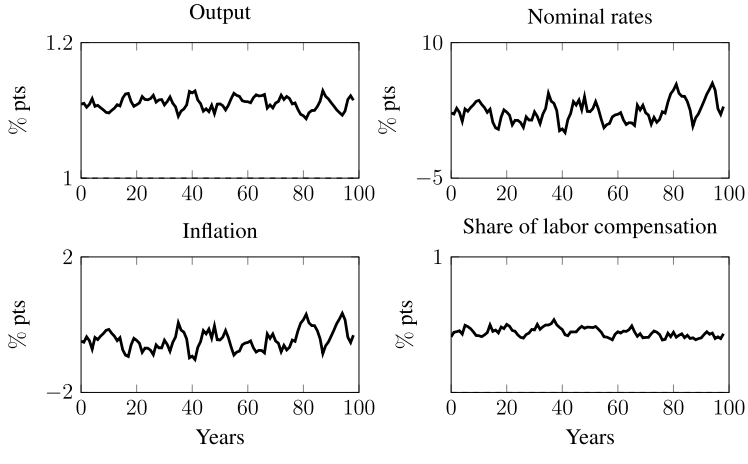

FIGURE 13.—Simulated paths for aggregate variables using the calibrated competitive equilibrium.

TABLE VII

DISTRIBUTIONAL MOMENTS ALONG THE PATH.

Moments	Data	Model			
		$t = 10$	$t = 25$	$t = 50$	$t = 75$
Std. share of equities	2.63	2.62	2.62	2.62	2.62
Std. bond	6.03	6.18	6.46	7.06	7.31
Std. ln wages	0.80	0.81	0.81	0.80	0.80
Std. ln hours	0.42	0.42	0.45	0.49	0.51
Corr(share of equities, ln wages)	0.40	0.37	0.33	0.27	0.22
Corr(share of equities, bond holdings)	0.62	0.59	0.50	0.33	0.22
Corr(bond, ln wages)	0.33	0.40	0.44	0.48	0.50

Note: The data moments correspond to SCF 2007 wave with sample restrictions explained in the text and after scaling wages, equity holdings, and debt holdings by the average yearly wage in our sample. The share of equities refers to the ratio of individual equity holdings to the total in our sample such that the weighted sum of shares equals one. The model columns correspond to simulated sample of 100,000 agents using the baseline calibration from Section 4.

$t \in \{10, 25, 50, 75\}$. Here, we notice a small drift in the distribution of the risk-free assets. The more significant drifts are in the correlations of of log wages and dividend shares as well as risk-free assets and dividend shares, which steadily declines over time and the correlation between bonds and log wages that increase over time. These patterns are the outcomes of the features in the baseline that claims to equity are not traded and households are subject to natural debt limits.

APPENDIX C: ADDITIONAL DETAILS FOR SECTION 5

C.1. *Cyclical Properties of Optimal Policies*

In this section, we present the counterpart of Table III in the main text for two intermediate economies between our baseline HANK and RANK: (i) first, we turn off the idiosyncratic shocks, and (ii) then we additionally allow agents trade a full set of Arrow securities. In the top panel of Table VIII, we see that the moments are very similar between the baseline HANK and the HANK with no idiosyncratic risk. In the bottom panel of Table VIII, we see that HANK with complete markets is quite similar to RANK, and very different from either the baseline HANK or the HANK with no idiosyncratic risk. From this, we can deduce that optimal policies are driven mainly by how much of the aggregate shocks agents can hedge using private markets.

C.2. *Example With Perfectly Aligned Distribution of Equity Shares*

As noted in Section 6.1, the quantitative driver of the need for insurance concerns against the markup shocks is the misalignment of dividend income from labor income. To illustrate this point, we construct a calibration with a nontrivial amount of inequality but in which these shares are perfectly aligned. To achieve this, we take the distribution of labor productivities from the benchmark calibration; assume Pareto weights such that optimal tax rates $\bar{\Upsilon}$ equal zero; and then assign dividend shares such that individuals initial share of labor income $\frac{\epsilon_{i,o} n_{i,0}}{\int_i \epsilon_{i,0} n_{i,0}}$ equals their share of dividend income s_i. Figure 14 plots the

TABLE VIII

MOMENTS.

	HANK					HANK No Idiosyncratic				
	Std. Dev (%)	Correlations				Std. Dev (%)	Correlations			
		i_t	Π_t	W_t	$\ln Y_t$		i_t	Π_t	W_t	$\ln Y_t$
Nominal rate i_t	1.82	1				1.50	1			
Inflation Π_t	0.46	−0.94	1			0.41	−0.93	1		
Labor share W_t	2.13	−0.78	0.78	1		1.83	−0.69	0.73	1	
Log output $\ln Y_t$	0.88	−0.31	0.10	0.12	1	0.82	−0.31	0.02	0.04	1

	HANK Complete Markets					RANK				
	Std. Dev (%)	Correlations				Std. Dev (%)	Correlations			
		i_t	Π_t	W_t	$\ln Y_t$		i_t	Π_t	W_t	$\ln Y_t$
Nominal rate i_t	0.87	1				0.87	1			
Inflation Π_t	0.03	0.01	1			0.03	−0.01	1		
Labor share W_t	1.20	−0.14	−0.25	1		1.18	−0.09	−0.32	1	
Log output $\ln Y_t$	0.92	−0.98	−0.1	0.30	1	0.92	−0.98	−0.09	0.24	1

Note: Moments are computed using allocations under HANK (top left); HANK without idiosyncratic shocks (top right); HANK with complete markets (bottom left); and RANK (bottom right) optimal monetary policies.

optimal response and its when the shares are aligned. We see that the alignment of shares nearly removes all need for insurance bringing the policy responses in line with those of the representative agent.[41]

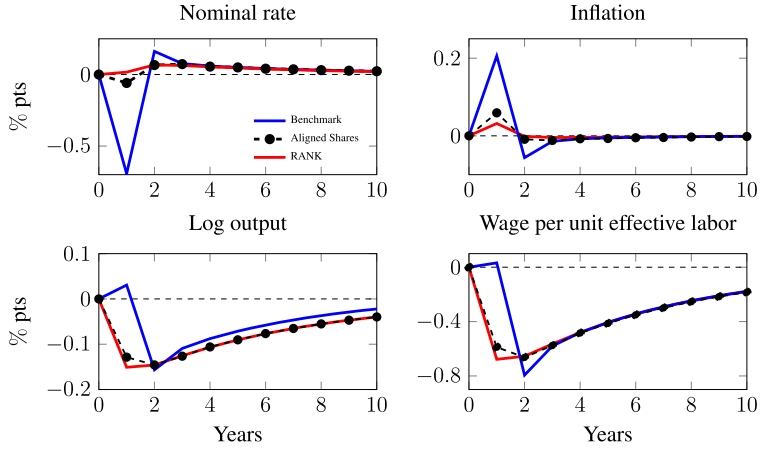

FIGURE 14.—Optimal monetary response to a markup shock. The bold blue and red lines are the calibrated HANK and RANK responses, respectively. The dashed black lines with circles are responses under HANK when the shares of labor and dividend income are aligned.

[41]There is some difference in insurance needs arising from differential labor responses to the markup shock.

APPENDIX D: ADDITIONAL DETAILS FOR SECTION 6

In the main body, we focused on the results under the baseline calibration and briefly discuss sensitivity checks and special cases. In this section, we provide all the omitted details.

D.1. *Sensitivity With Respect to Price Adjustment Costs*

In this section, we present the impulse responses under alternative choices for the price adjustment cost parameter ψ. As mentioned in Section 6.1, we vary ψ from twice the baseline calibration to one quarter of the baseline calibration, and also when ψ is approximately zero. Figure 15 plots the responses to a markup shock while Figure 16 plots responses to a productivity shock.

As is readily apparent in both figures, the effect on inflation is roughly linear for a large range of ψ. Doubling ψ leads to a halving of inflation while halving ψ leads to a doubling of inflation. The effect on the nominal rate is quite small. In the limit as ψ approaches zero, the planner can no longer effect real variables through monetary policy and instead relies more on unexpected inflation to provide insurance through the ex post real return as instead of distorting the allocation by varying the ex ante real rate.

D.2. *Sensitivity With Respect to Choice of Pareto Weights*

Here, we present sensitivity to the choice of Pareto weights. As mentioned in the main text, we set Pareto weights using a thee parameter exponential specification, which loads on the three dimensions of initial heterogeneity and maps to optimal levels of tax rates $\bar{\Upsilon}$, on labor income, dividend income, and bond income. For the purpose of sensitivity, we vary these implied tax rates in a large range: from 0% to 50%. In addition, we also study a Utilitarian planner that weights all agents equally.

We start with the experiments that vary the labor income tax rate and the responses are depicted in Figures 17 and 18 to markup and productivity shocks, respectively. We

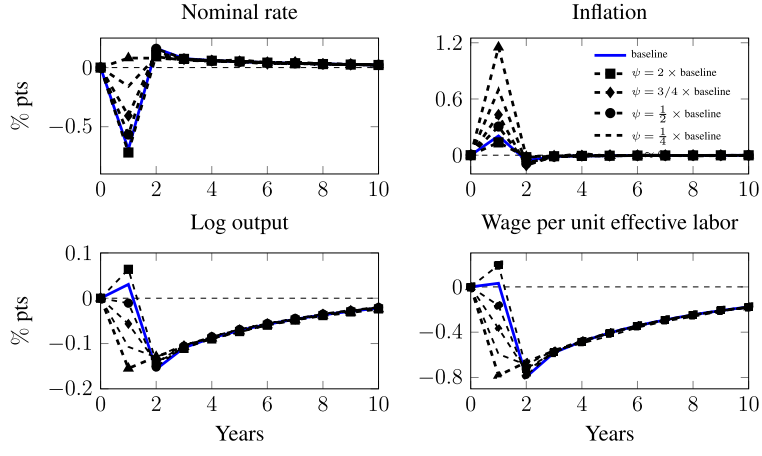

FIGURE 15.—Optimal monetary response to a markup shock. The bold blue lines are the responses for the baseline calibration. The dashed black lines with squares, circles, and triangles are responses under a calibration in which we double the price adjustment costs parameter, half the price adjustment cost parameter, and finally set it near zero, respectively.

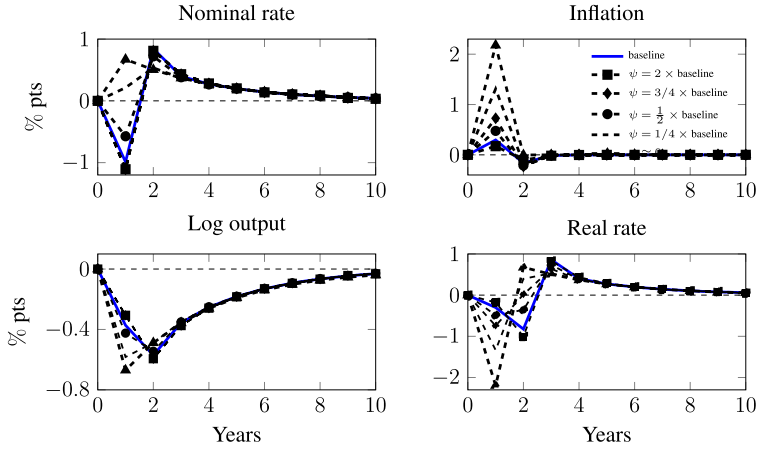

FIGURE 16.—Optimal monetary response to a TFP shock. The bold blue lines are the responses for the baseline calibration. The dashed black lines with squares, circles, and triangles are responses under a calibration in which we double the price adjustment costs parameter, half the price adjustment cost parameter, and finally set it near zero, respectively.

see that the responses to both the shocks are larger when labor tax rates are higher and lower when labor taxes are lower. Raising the labor tax compresses labor shares pushing the economy further away from full insurance, while decreasing the labor tax pushes the economy closer to full insurance. In line with this, we see that the increasing the labor tax leads to a stronger policy response while decreasing the labor tax diminishes the response.

Next, we vary the tax on dividend income and report the results in Figures 19 and 20. Our baseline calibration exhibits are far more unequal distribution of dividend share than labor shares. Increasing the dividend tax brings the economy closer to full insurance while decreasing the dividend tax pushes the economy away from full insurance. As such, we see that the response of inflation and other variables is stronger when the dividend tax is low

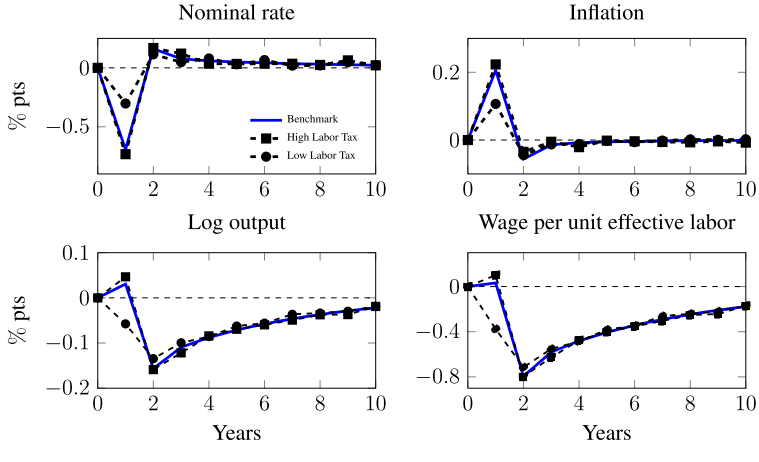

FIGURE 17.—Optimal monetary response to a markup shock with alternative Pareto weights. The bold blue lines are the responses for the baseline calibration. The dashed black lines with squares and circles are responses under a calibration with higher and lower labor taxes respectively.

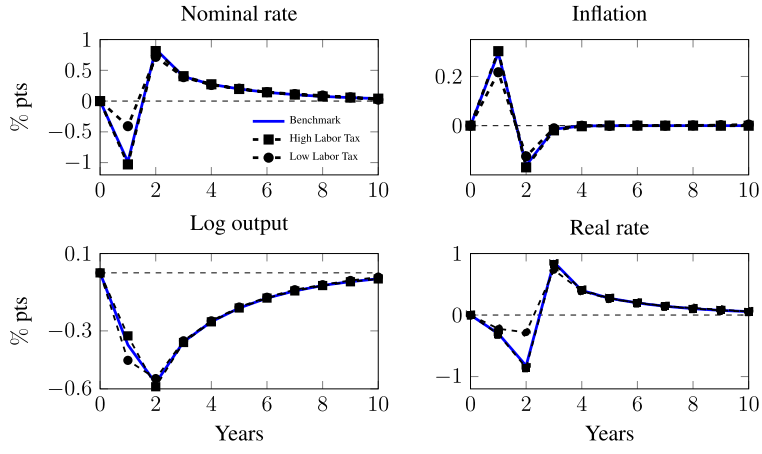

FIGURE 18.—Optimal monetary response to a TFP shock for alternative Pareto weights. The bold blue lines are the responses for the baseline calibration. The dashed black lines with squares and circles are responses under a calibration with higher and lower labor taxes respectively.

and weaker when it is high when we look at markup shocks. Since productivity shocks affect wages and dividends symmetrically, we should expect that the responses are not very different across cases that vary in the level of tax on dividend income. This prior is confirmed in Figure 20.

On the contrary, a bond tax directly controls the dispersion in after-tax bond income, which is key statistic for insurance against a productivity shock. In Figures 21 and 22, we see that a higher bond tax lowers the response to the productivity shock and leaves the response to markup shock barely unchanged. To make our plots comparable with the baseline case, we report impulse responses to the after-tax nominal and real interest rates.

Finally, we study the utilitarian planner who sets Pareto weights equal. In our setup, a utilitarian planner would set labor tax rate of 68%, a dividend tax rate of 116%, and a

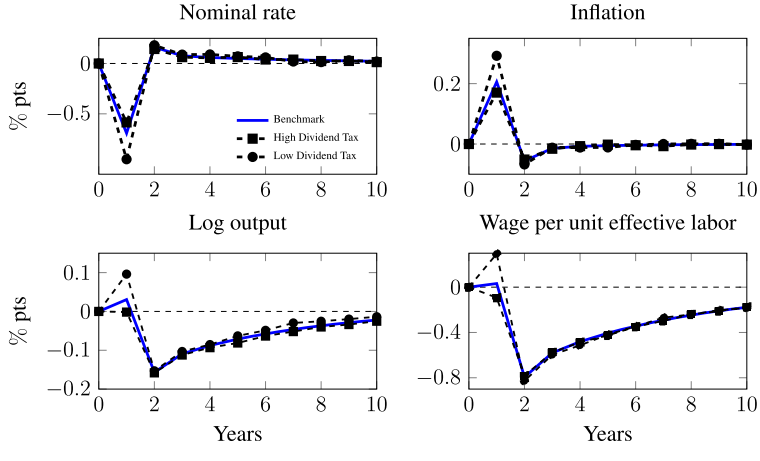

FIGURE 19.—Optimal monetary response to a markup shock for alternative Pareto weights. The bold blue lines are the responses for the baseline calibration. The dashed black lines with squares and circles are responses under a calibration with higher and lower dividend taxes respectively.

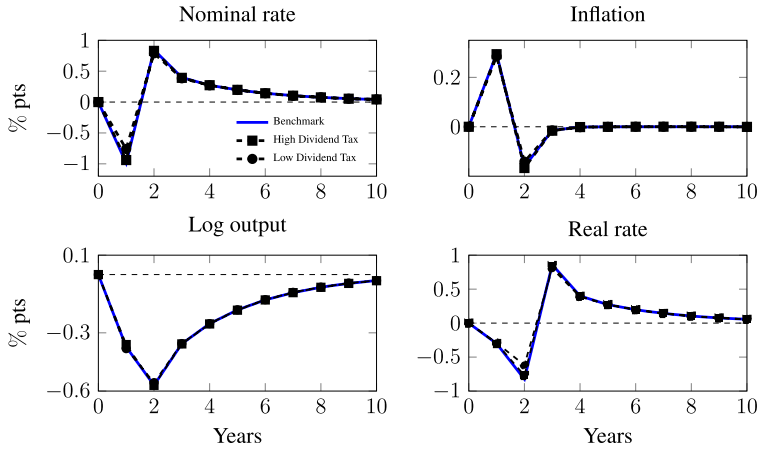

FIGURE 20.—Optimal monetary response to a TFP shock for alternative Pareto weights. The bold blue lines are the responses for the baseline calibration. The dashed black lines with squares and circles are responses under a calibration with higher and lower dividend taxes respectively.

bond tax rate of 118%. These effects go in offsetting directions but overall we find little deviation from the baseline responses. The results are summarized in Figures 23 and 24.

D.3. *Sensitivity With Respect to the Period of the Shock*

In this section, we compare optimal responses to a shock that occurs at $t = 25$ as well as $t = 50$ with our baseline in which the shocks occur at $t = 1$. For brevity, we only report the optimal monetary response. Figure 25 plots the response to a markup shock, and Figure 26 plots a response to a TFP shock. We find the responses to be very similar. The response to the TFP shock are slightly larger with time because the distribution of risk-

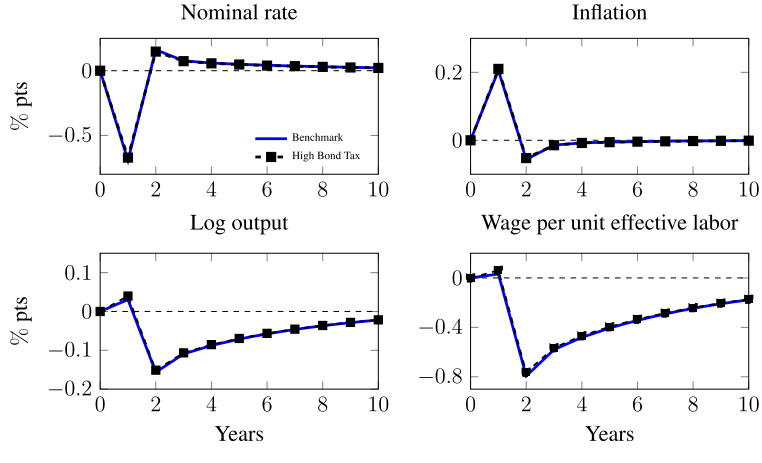

FIGURE 21.—Optimal monetary response to a markup shock with alternative Pareto weights. The bold blue lines are the responses for the baseline calibration. The dashed black lines with squares are responses under a calibration with higher bond taxes.

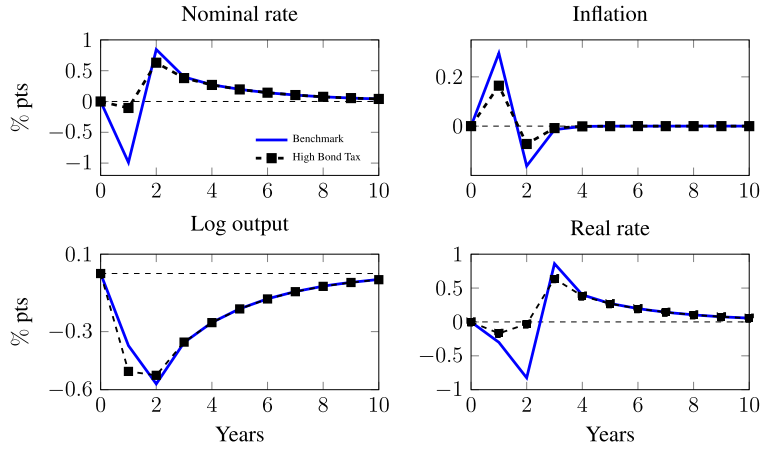

FIGURE 22.—Optimal monetary response to a TFP shock for alternative Pareto weights. The bold blue lines are the responses for the baseline calibration. The dashed black lines with squares are responses under a calibration with higher bond taxes.

free debt spreads out with idiosyncratic shocks and, therefore, there is a larger role for providing insurance.

D.4. *Sensitivity With Respect to Choice of Initial Conditions*

In the main text, we set the initial distribution of productivities, risk-free nominal bonds claims, and equity claims using the observed SCF distribution. Here, we redo the optimal policy starting at a joint distribution of wealth and productivities that arises after simulating 100 years in the calibrated competitive equilibrium with fixed policies. The results are summarized in Figures 27 and 28. The response to a markup shock is a balance of two forces. On the one hand, the passage of time diminishes the correlation between stock

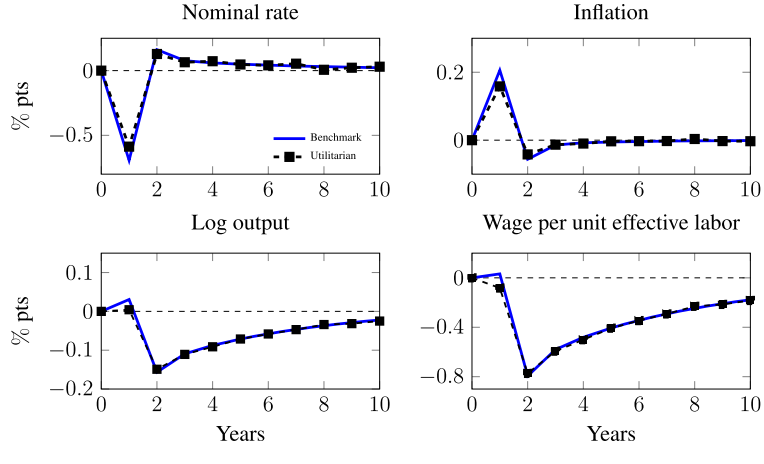

FIGURE 23.—Optimal monetary response to a markup shock for utilitarian Pareto weights. The bold blue lines are the responses for the baseline calibration. The dashed black lines with squares are responses under utilitarian Pareto weights.

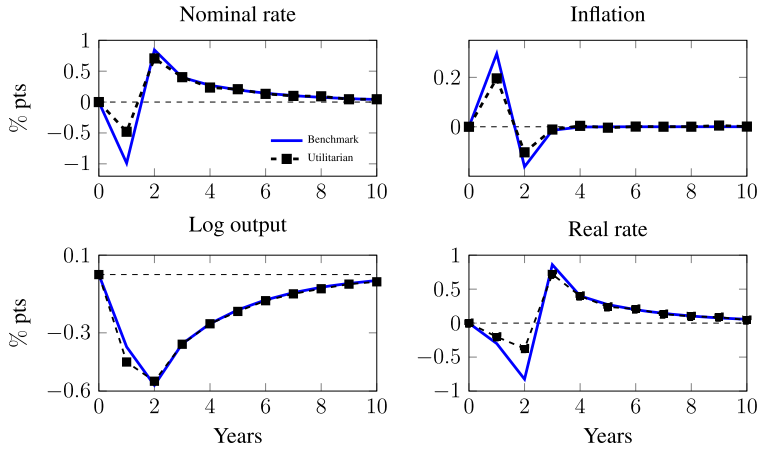

FIGURE 24.—Optimal monetary response to a TFP shock for utilitarian Pareto weights. The bold blue lines are the responses for the baseline calibration. The dashed black lines with squares are responses under utilitarian Pareto weights.

holdings and labor earnings, which renders inequality more misaligned according to our distance measure. That increases the planner's gains from providing insurance. On the other hand, the correlation of shares of equities and bond holdings diminishes, which diminishes the insurance gains from the unanticipated inflation. The increase in the spread of nominal debt leads the planner to be more responsive to a TFP shock.

D.5. *Example With Poor Hand-to-Mouth Agents*

We can also consider an alternative calibration of the hand-to-mouth agents where we restrict bottom 15% of the cash-in-hand distribution to be hand-to-mouth. This environment is similar in spirit to what would arise in an standard Aiyagari model as the new

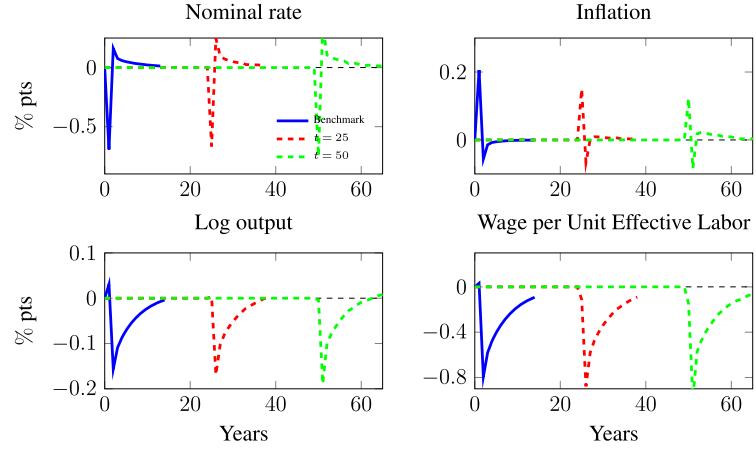

FIGURE 25.—Optimal monetary response to a markup shock for alternative initial conditions. The bold blue lines are the responses for the baseline calibration. The dashed lines are from the policies after initializing the the Ramsey allocation with $t = 1, 25, 50$ years of the competitive equilibrium.

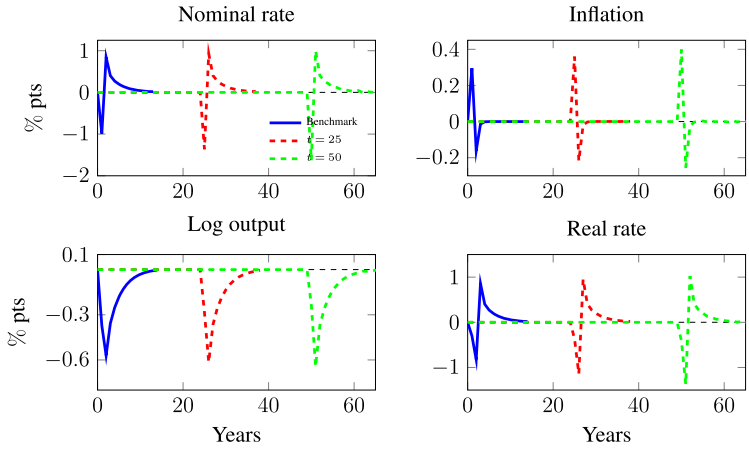

FIGURE 26.—Optimal monetary response to a TFP shock for alternative initial conditions. The bold blue lines are the responses for the baseline calibration. The dashed lines are from the policies after initializing the the Ramsey allocation with $t = 1, 25, 50$ years of the competitive equilibrium.

hand-to-mouth agents more homogeneous and are almost entirely reliant on labor income. We plot the optimal policy response with only poor hand-to-mouth agents using the dashed red line in Figure 29. As opposed to the hand-to-mouth setting in the main text that is calibrated to the evidence in Jappelli and Pistaferri (2014), the optimal policy with only poor hand to mouth agents is almost identical to that of the baseline economy as the government can construct a transfer scheme to smooth the consumption of the hand to mouth agents by mirroring the path of wages.

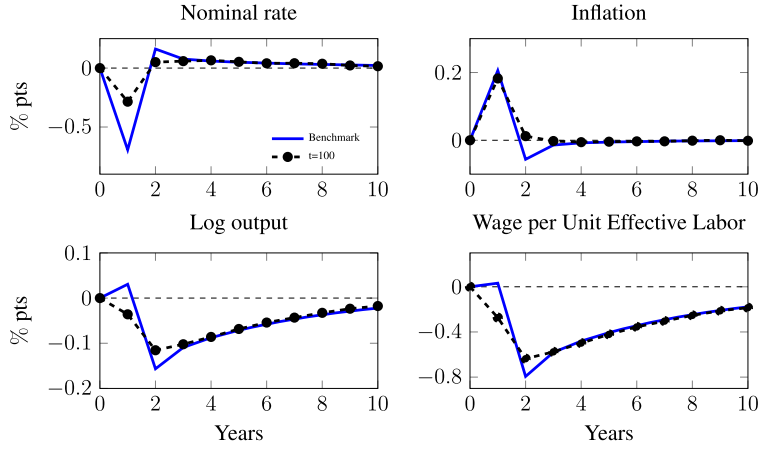

FIGURE 27.—Optimal monetary response to a markup shock for alternative initial conditions. The bold blue lines are the responses for the baseline calibration. The dashed lines are from the policies after initializing the the Ramsey allocation with $t = 100$ years of the competitive equilibrium.

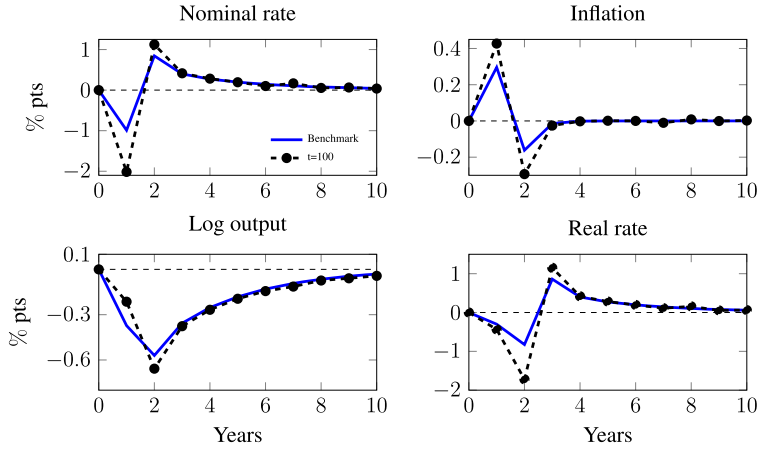

FIGURE 28.—Optimal monetary response to a TFP shock for alternative initial conditions. The bold blue lines are the responses for the baseline calibration. The dashed lines are from the policies after initializing the the Ramsey allocation with $t = 100$ years of the competitive equilibrium.

D.6. *Heterogeneous Marginal Propensity to Consume From Dividend Income and Wage Income*

In this section, we study optimal monetary responses in a variant in which liquidity constrained agents can smooth dividend income. This results in a lower marginal propensity to consume out of income from capital income relative to income from labor. To model this, we change the savings rule for agents with the $h_i = 1$ from $P_t Q_t b_{i,t} = P_0 Q_0 b_{i,0}$ to

$$P_t Q_t b_{i,t} = P_0 Q_0 b_{i,0} + s_i P_t \tilde{D}_t,$$
$$\tilde{D}_t = \tilde{D}_{t-1} + (1 - \text{divMPC}) \times (D_t - \overline{D}_t),$$

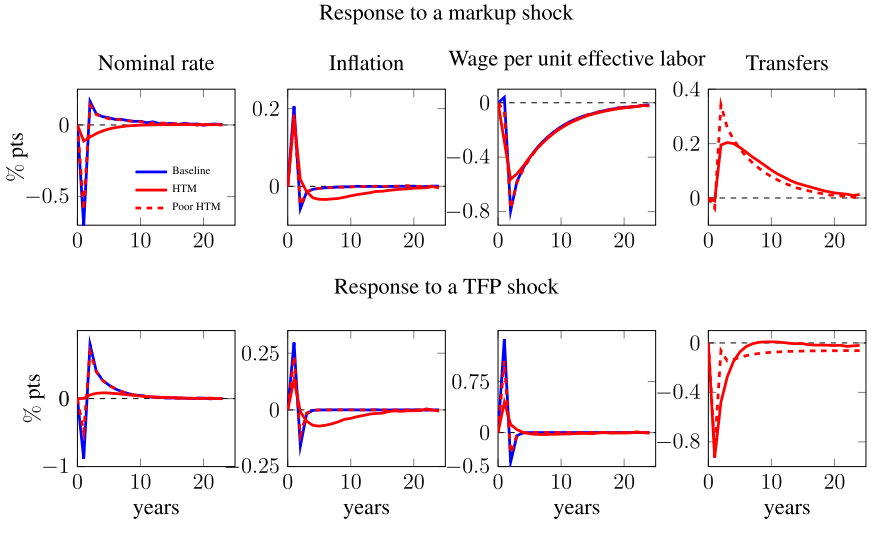

FIGURE 29.—Optimal monetary responses with hand-to-mouth agents. The top panel plots responses to a markup shock and the bottom panel plots responses to a productivity shocks.

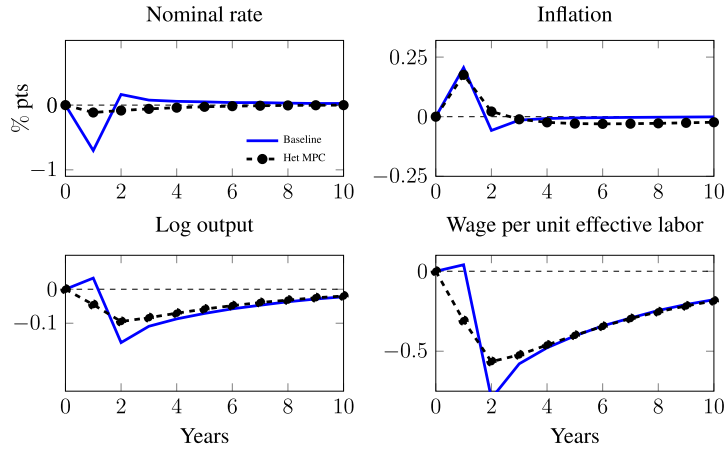

FIGURE 30.—Optimal monetary responses to the markup shock with heterogeneous marginal propensities to consume. The bold blue lines are responses under the baseline and the dashed black lines with circles are responses with heterogeneous marginal propensities to consume out of dividend and labor incomes.

where $\bar{D}_t$ is the long run dividend level. The state variable $\tilde{D}_t$ is similar to holdings of mutual fund in which households save the fluctuations in their dividend income and are paid at a risk-free on the balance in return. For the rest of the section, we set divMPC $= 0$. In Figures 30 and 31, we plot optimal monetary responses to the markup and the productivity shock, respectively.

As we describe in the main text in Section 6.2, heterogeneity in marginal propensity to consume across households makes the path of the optimal interest rate smoother. Manipulating the timing of lump sum transfers is not sufficient to insure the consumption path of the constrained agents who differ in their holdings on stocks and bonds. The planner uses monetary policy to directly smooth real returns and wages. While implementing such smoothing, there is a tension: smoothing the wage and dividend share that helps

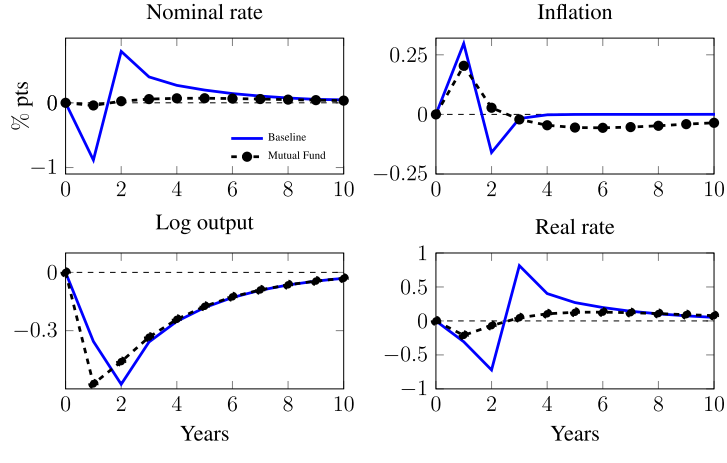

FIGURE 31.—Optimal monetary responses to productivity shock with heterogeneous marginal propensities to consume. The bold blue lines are responses under the baseline and the dashed black lines with circles are responses with heterogeneous marginal propensities to consume out of dividend and labor incomes.

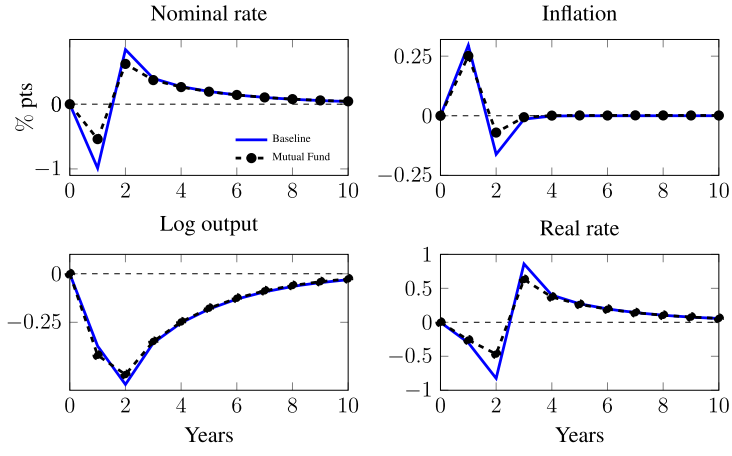

FIGURE 32.—Optimal monetary responses to productivity shock with mutual fund. The bold blue lines are responses under the baseline and the dashed black lines with circles are responses under the mutual fund setting.

liquidity constrained stockholders requires movements in natural rates that hurt liquidity constrained bond holders. Allowing for the ability to additionally smooth dividends relaxes this tension and the results in paths of nominal rates that are even more smooth. Quantitatively, this effect is larger for markup shocks than for productivity shocks.

D.7. *Optimal Monetary-Fiscal Response With Mutual Fund*

In this section, we present optimal monetary response to productivity shock, as well as the optimal monetary-fiscal response to both under the mutual fund calibration. The optimal monetary response to the productivity shock is in Figure 32.

One aspect of the mutual fund calibration is that it enforces a perfect correlation between bond and dividend wealth following any history of shocks. As a result, the optimal policy the bond and dividend tax rates are indeterminate as the planner can achieve the same effective returns with either instrument. To make the results comparable with our benchmark calibration, we assume that the planner adjusts the dividend tax in response to a markup shock and the bond rate in response to a markup shock. The results are plotted in Figures 33 and 34. In both cases, the optimal policy under the mutual fund is almost identical to the benchmark calibration.

D.8. *Optimal Monetary and Monetary-Fiscal Response to a TFP Shock With Heterogeneous Labor Income Exposures*

As noted in Section 6.4, we calibrate the coefficients of $f(\theta) = f_0 + f_1\theta + f_2\theta^2$ by simulating the competitive equilibrium for 30 periods and extracting "recessions" as consecutive periods where the growth rate of output one standard deviation below zero. Following the empirical procedure in Guvenen, Ozkan, and Song (2014), we rank workers by percentiles of their average log labor earnings 5 years prior to the shock and compute the percent earnings loss for each percentile relative to the median. The parameters f_1, f_2 are set to match earnings losses of the 5th, 95th percentiles. The parameter f_0 is set so that agent with the median productivity faces a drop similar to the aggregate TFP. Figure 35

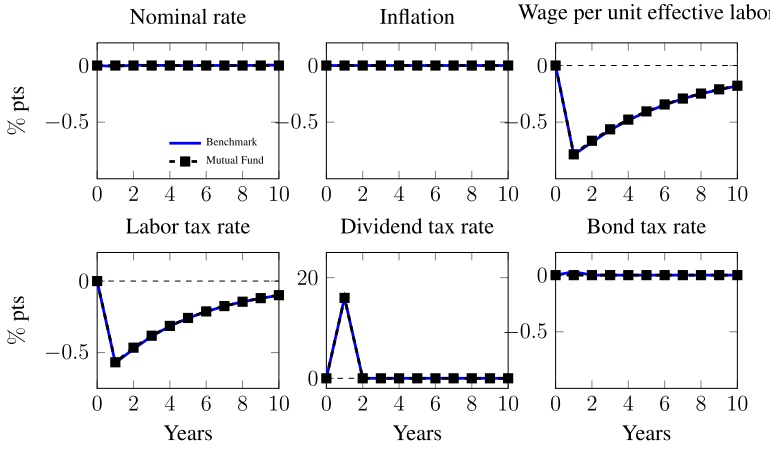

FIGURE 33.—Optimal monetary-fiscal response to a markup shock with the mutual fund. The bold red are the benchmark response while the bold blue lines are the responses for the mutual fund calibration.

plots the earnings losses by percentile of the income distribution relative to those found by Guvenen, Ozkan, and Song (2014).

Figure 36 plots the responses of the monetary-fiscal policy. When the government has access to fiscal policy, it no longer needs to rely solely on monetary policy. In Figure 36, we see that in response to an inequality shock the planner raises the labor tax rate by nearly 1% and then allows it to mean revert back as the TFP shock dissipates. This mean reversion arises because the level of inequality loads on TFP and partly captures the forces laid out in Werning (2007) where the planner responds to changes in relative labor productivity though changes in the labor tax rate. Unlike in the baseline case when nearly all insurance can be provided through a surprise tax on bond income, the planner must also rely on a surprise increase in the dividend tax rate to partially provide insurance. This highlights a feature of heterogeneous agent models. Unlike representative agent models where a single tax on returns can complete markets, with heterogeneous agents one tax

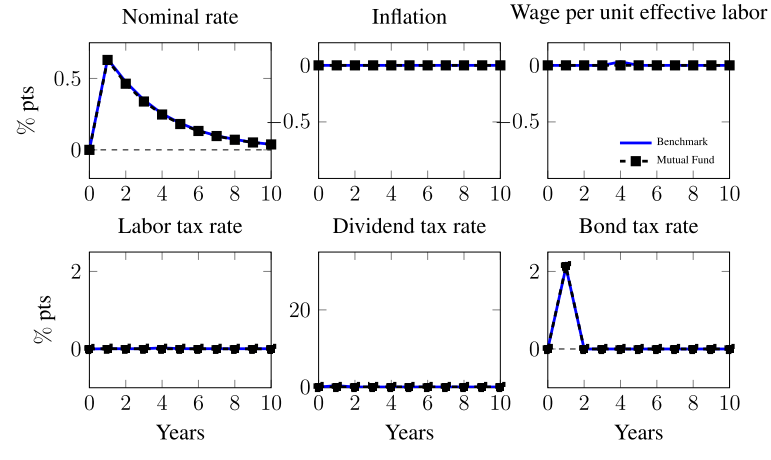

FIGURE 34.—Optimal monetary-fiscal response to a TFP shock with mutual fund. The bold blue lines are the response under the baseline while the dashed black lines are the responses for the mutual fund calibration.

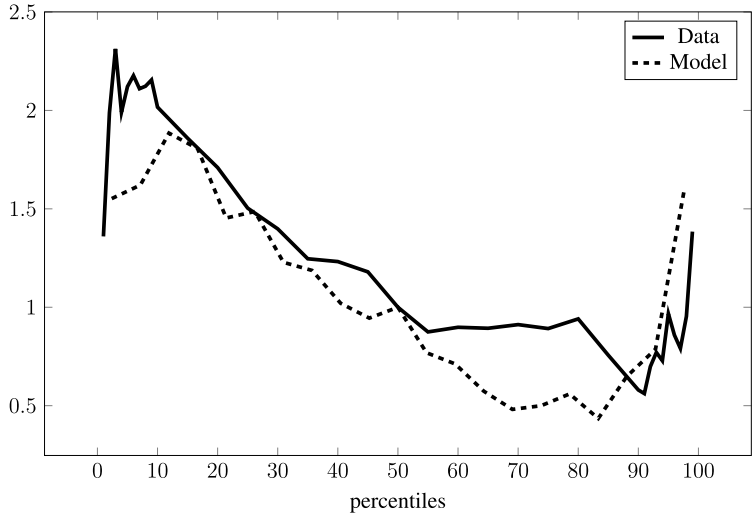

FIGURE 35.—Relative income losses after recessions in data (solid line) and model (dashed line).

may not provide insurance for all agents and the planner may exploit multiple different asset taxes.

In Figure 37, we apply our decomposition to the monetary response with setting with heterogeneous exposures. The small difference in the rate of inflation in the HANK complete market relative to RANK case captures the redistribution. In Figure 36, we saw that labor income taxes are used to respond to inequality even with complete markets. When the planner cannot adjust labor income tax, wages and thereby inflation is used to attain similar objectives.

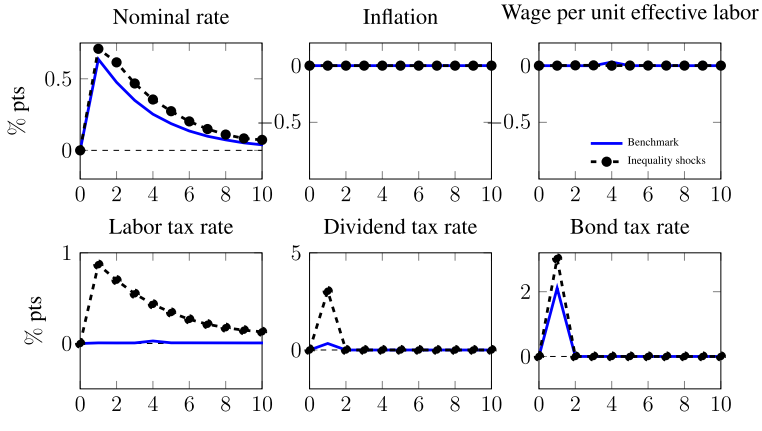

FIGURE 36.—Optimal monetary-fiscal response to a TFP shock with heterogeneous income exposures. The bold blue lines are the response under the baseline calibration while the dashed black lines are the responses calibration with heterogeneous exposures to TFP shocks.

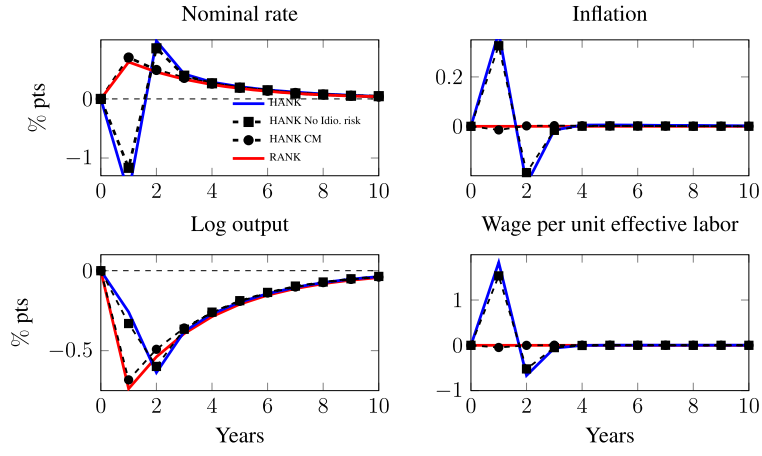

FIGURE 37.—Decomposition of the optimal monetary response to a TFP shock with heterogeneous exposures. The bold blue and red lines are the calibrated HANK and RANK responses, respectively. The dashed black lines with squares and circles are responses under HANK with idiosyncratic shocks shutdown and with complete markets, respectively.

REFERENCES

ACHARYA, S., AND K. DOGRA (2018): "Understanding HANK: Insights From a PRANK," FRB of New York Staff Report No. 835. [18,19]

DOEPKE, M., AND M. SCHNEIDER (2006): "Inflation and the Redistribution of Nominal Wealth," *Journal of Political Economy*, 114 (6), 1069–1097. [23]

GUVENEN, F., S. OZKAN, AND J. SONG (2014): "The Nature of Countercyclical Income Risk," *Journal of Political Economy*, 122 (3), 621–660. [36,37]

HUGGETT, M. (1993): "The Risk-Free Rate in Heterogeneous-Agent Incomplete-Insurance Economies," *Journal of Economic Dynamics and Control*, 17 (5), 953–969. [22]

JAPPELLI, T., AND L. PISTAFERRI (2014): "Fiscal Policy and MPC Heterogeneity," *American Economic Journal: Macroeconomics*, 6 (4), 107–136. [33]

WERNING, I. (2007): "Optimal Fiscal Policy With Redistribution," *Quarterly Journal of Economics*, 122, 925–967. [37]

Co-editor Giovanni L. Violante handled this manuscript.

Manuscript received 6 June, 2018; final version accepted 20 March, 2021; available online 30 April, 2021.